10.15774/PPKE.ITK.2024.001

Development of Brain-Computer Interfaces by using Deep Learning Technologies

Csaba Márton Köllőd

Pázmány Péter Catholic University
Faculty of Information Technology and Bionics
Roska Tamás Doctoral School of Sciences and Technology

Supervisor: István Ulbert, DSc

A thesis submitted for the degree of *Doctor of Philosophy*

Budapest, 2023

10.15774/PPKE.ITK.2024.001

Abstract

The development of real-time Brain-Computer Interface (BCI) Systems, capable of controlling external digital devices or computer games, requires the integration of multiple scientific fields, ranging from electrophysiology to signal processing, artifact detection, feature extraction, and classification using artificial intelligence-based methods.

In the first thesis group, I present a comprehensive development pathway for a BCI system, proposing a combination of feature extraction and classification algorithms with low computational requirements. I compared the developed range40 feature extraction method, in conjunction with my Voting SVM, to the state-of-the-art EEGNet classifier and I demonstrated superior classification accuracy. Additionally, I propose a novel Toggle Switch control mechanism that can expand two control classes to four or more control signals. I successfully implemented these algorithms in experiments where tetraplegic subjects played a car racing computer game using only mental commands.

In the second thesis group, I conducted a comparative analysis of five renowned neural networks (Shallow ConvNet, Deep ConvNet, EEGNet, EEGNet Fusion, and MI-EEGNet) using open-access databases with larger subject pools. My objective was to underscore the limitations of databases that encompass MI EEG data from a limited number of subjects (typically ≤ 10) without advanced artifact filtering methods. I also demonstrate that transfer learning can enhance the classification accuracy of selected networks even after artifact filtering preprocessing of EEG data. As a final contribution, I present two metrics that reveal the insufficiency of relying solely on neural network accuracy for ranking purposes. Earlier members of the EEGNet family, such as Shallow ConvNet and Deep ConvNet, can outperform later published members concerning accuracy improvement from chance level and the effect of transfer learning metrics.

10.15774/PPKE.ITK.2024.001

Összefoglaló

A valós idejű Agy-Számítógép Kapcsolat (angolul: Brain-Computer interface, továbbiakban: BCI) rendszerek fejlesztéséhez, amelyek képesek külső digitális eszközök vagy számítógépes játékok vezérlésére, több tudományos terület integrációja szükséges, az elektrofiziológiától a jel feldolgozáson, az artefakt detektáláson, valamint a jellemző kinyerésen át a mesterséges intelligencia-alapú osztályozásig.

Az első téziscsoportban egy átfogó fejlesztési utat mutatok be egy BCI rendszer számára, javasolva egy jellemzőkinyerési és osztályozási algoritmus kombinációt, amely alacsony számítási kapacitást igényel. A range40 jellemzőkinyerési módszert a Voting SVM-mel kombinálva összevetettem a legmodernebb EEGNet osztályozóval, melynél jobb osztályozási pontosságot értem el. Továbbá javaslatot teszek egy új Váltó Kapcsoló vezérlési mechanizmusra, amely képes két vezérlőosztályt négy vagy több vezérlőjelre bővíteni. Ezeket az algoritmusokat sikeresen alkalmaztam valós idejű kísérletek során, ahol tetraplegiás alanyok autóverseny-szerű számítógépes játékot játszottak kizárólag mentális utasítások segítségével.

A második téziscsoportban összehasonlító elemzést végeztem öt neves neurális hálózatról (Shallow ConvNet, Deep ConvNet, EEGNet, EEGNet Fusion és MI-EEGNet) nyílt hozzáférésű adatbázisokfelhasználásával, melyek nagyszámú kísérleti alanyok bevonásával készültek. Célom volt, hogy hangsúlyozzam azoknak az adatbázisoknak a korlátait, melyek elképzelt motoros mozgatásos EEG adatokat tartalmaznak korlátozott számú alanytól (általában ≤ 10), haladó zajszűrési módszerek használata nélkül. Bemutatom azt is, hogy a transzfer tanulás javíthatja a kiválasztott hálózatok osztályozási pontosságát még az EEG adatok artefakt szűrése után is. Végül bemutatok két metrikát, melyek szemléltetik, hogy kizárólag a neurális hálózatok pontosságának figyelembevétele nem elegendő a rangsorolásukhoz. Az EEGNet család idősebb tagjai, mint például a Shallow ConvNet és a Deep ConvNet, le tudják hagyni a később publikált leszármazottaikat a következő metrikák alkalmazása mellett: véletlen szinttől való pontosságjavulás és a transzfer tanulás hatása.

10.15774/PPKE.ITK.2024.001

Contents

10.15774/PPKE.ITK.2024.001

List of Abbreviations

AIS	Asia Impairment Scale
ANN	Artificial Neural Network
AP	Action Potential
BCI	Brain-Computer Interface
CNN	Convolutional Neural Network
CSP	Common Spatial Pattern
CWT	Continuous Wavelet Transformation
DWT	Discrete Wavelet Transformation
ECoG	Electrocorticography
EEG	Electroencephalography
EOG	Electrooculogram
FASTER	Fully Automated Statistical Thresholding algorithm
FBCSP	Filter Bank Common Spatial Pattern
FFT	Fast Fourier Transform
FFTabs	absolute value of the Fast Fourier Transformation
GoPar	General Offline Paradigm
IC	Independent Component
ICA	Independent Component Analysis
LDA	Linear Discriminant Analysis
LFP	Local Field Potential
LSL	Lab Streaming Layer
MAV	Mean Absolute Value
MEG	Magnetoencephalography
MI	Motor Imagery
MUA	Multi Unit Activity
NLI	Neurological Level of Injury

PSD	Power Spectral Density
RBF	Radial-Basis-Function
RCSP	Regularized CSP
RMS	Root Mean Square
SMR	Sensory Motor Rhythm
SSC	Slope Sign Changes
STFT	Short Time Fourier Transformation
SUA	Single Unit Activity
SVM	Support Vector Machine
TTK	Research Centre for Natural Sciences
VEP	Visual Evoked Potential
c-VEP	code-modulated VEP
f-VEP	frequency-modulated VEP
t-VEP	time-modulated VEP
WL	Waveform Length
WT	Wavelet Transform
ZC	Zero Crossing

10.15774/PPKE.ITK.2024.001

Acknowledgements

If it weren't for the last minute, nothing would be finished. Therefore, I would like to express my deepest gratitude to my supervisor, István Ulbert, who, despite his busy schedule, was always available and ready to provide valuable feedback and guidance on my work.

Great colleagues are essential for the successful completion of experiments and studies. I am grateful to András Adolf for his dedication in co-conducting the experiments and assisting me in the development of the BCI System. I also extend my thanks to Gergely Márton for accepting the role of industrial supervisor for my KDP grant and for providing insightful comments and feedback on my manuscripts. Ward Fadel and Moutz Wahdow also provided invaluable assistance during the experiments.

The Cybathlon would not have been possible without the participation of our pilots. I have great respect for B. Zoli and Csorti, who willingly applied for this task and participated weekly in the experiments. We also shared many enjoyable moments together. I would like to extend my thanks to MEREK, the Rehabilitation Centre for Physically Disabled People in Hungary, for providing us with a room where we could organize our weekly experiments. Support from the University came in the form of Kristóf Iván, who equipped us with a brand new BrainProducts EEG ActiChamp amplifier.

I am grateful for the financial and professional support provided by the Doctoral Student Scholarship Program of the Co-operative Doctoral Program (Hungarian abbreviation: KDP) of the Ministry of Innovation and Technology, financed by the National Research, Development and Innovation Fund (KDP-2021-12 1020483).

Last but not least, I would like to thank my wife, Bori, for her unwavering support and encouragement. Without you, I could not have overcome the challenges that life presented: Taking care of our 3 beautifully children, finding a new apartment and finishing this dissertation.

I dedicate my work to GOD, the greatest being in the Universe, who always guides me towards achieving the impossible.

10.15774/PPKE.ITK.2024.001

Chapter 1

Introduction

1.1. Motivation

Brain-Computer Interfaces (BCIs) represent a rapidly evolving interdisciplinary research field that holds significant potential for developing systems that allow individuals to communicate, control, and interact with technology using only their brain activity, bypassing the need for motor control or other physical input devices. This technology has the potential to greatly improve the quality of life for individuals with disabilities such as impaired vision, hearing, movement, or communication, and could be particularly beneficial for those with Locked In Syndrome, a condition resulting from illness or injury that prevents individuals from using their neuromuscular channels to move their body, despite being in a cognitively intact state.

However, despite the great potential of BCIs, there are still significant challenges to overcome. One of the main challenges is to improve the accuracy and reliability of the BCI systems, particularly in real-world scenarios with varying environments and user states. Additionally, BCIs based on communication systems may be significantly slower than traditional communication channels, but restoring the ability to communicate via these systems can have a profound impact on quality of life, irrespective of communication speed.

This dissertation aims to present a BCI System, which can be used by subjects with tetraplegia, to control a video game. In addition, it aims to investigate and compare different classification methods to further advance the field of BCI technology. The study involves the development of signal processing algorithms and machine learning models.

1.2. Overview of the Thesis

This section provides a brief overview of the present thesis. Chapter 2 offers a comprehensive background on the field of Brain-Computer Interfaces (BCIs), beginning with the source of the signal and progressing through the entire BCI system, highlighting each essential component required to construct a complete application capable of controlling an external digital device using mental commands.

Chapter 3 presents the first set of contributions, which focus on the development of a novel BCI system. Section 3.2.2.2 introduces the Feature Range feature extraction method, which employs Fast Fourier Transformation and combines it with an ensemble Support Vector Machine classification algorithm to classify Electroencephalography (EEG) signals. Section 3.2.6.1 details the Toggle Switch algorithm, designed to expand the number of control commands using the Two Choice Paradigm (Section 3.2.4). Section 3.3 presents the results of an offline comparison between our proposed system and the state-of-the-art EEGNet, as well as demonstrating the real-time usability of the BCI in gameplay experiments.

Chapter 4 concentrates on the classifier component of the BCI system and compares five renowned neural networks (Shallow ConvNet, Deep ConvNet, EEGNet, EEGNet Fusion, and MI-EEGNet) using open-access databases with a larger subject pool and the BCI Competition IV 2a dataset to obtain statistically significant results. The FASTER algorithm is employed as a signal processing step to eliminate artifacts from EEG data, and transfer learning is explored as a means of enhancing classification results on artifact-filtered data. The objective is to rank the neural networks; thus, in addition to classification accuracy, two supplementary metrics are introduced: accuracy improvement from chance level and the effect of transfer learning.

In Chapter 5, new scientific findings are summarized in the form of thesis points.

10.15774/PPKE.ITK.2024.001

Chapter 2

Background and Theory

Brain-Computer Interfaces are integrated systems comprising of software and hardware components that record bioelectrical signals from the brain. BCIs extract relevant information from the signal-noise mixture, and translate it into control commands for an external electric device, as explained by Wolpaw et al. [1]. Developing such a sophisticated system requires in-depth knowledge of electrophysiology, digital signal processing, classification algorithms, and programming. The BCI system consists of multiple parts, which must work coherently to generate accurate commands.

The sensor unit is a critical hardware component of BCI systems, which utilizes EEG to record bioelectrical signals. It consists of electrodes and an amplifier, which are responsible for detecting and amplifying the electrical signals. It also converts and digitizes bioelectrical signals for further processing. If an error occours in this input pipeline the rest of the BCI system practically unusable.

The software part of the system manages signal processing steps, including artifact filtering, feature extraction, and translation algorithms. The artifact filtering step aims to detect and eliminate noise from the signal-noise mixture. The feature extraction step enhances useful information from the purified signals, which can be employed for classification and reflects the user's mental state. Finally, the classification algorithm learns and classifies the generated features to generate proper device control commands. Figure 2.1 illustrates the structure of the BCI system described above. In the following the components of the BCI system is discussed in more detail.

10.15774/PPKE.ITK.2024.001

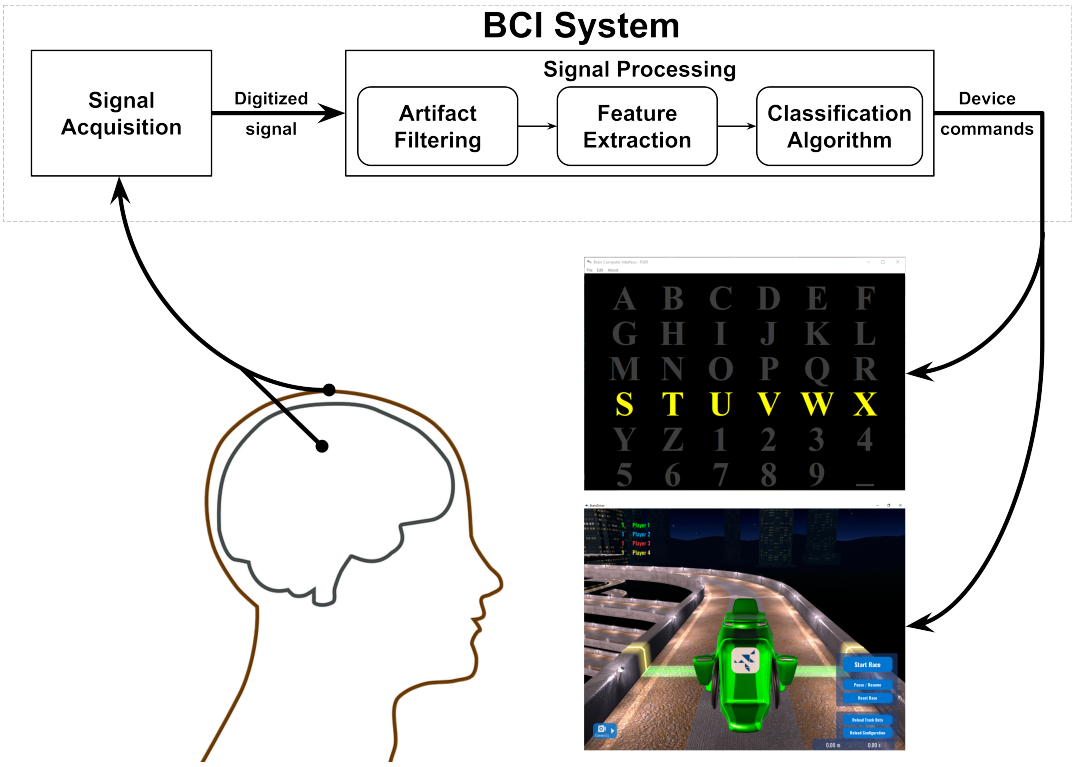

Figure 2.1. Components of a Brain-Computer Interface system

2.1. Signal Acquisition

2.1.1 The Source of the Signals – The Neuron

2.1.1.1 Structure

In the context of BCI applications, signals are generated by neurons within the Central Nervous System. As presented in Figure 2.2, a neuron comprises several key components [2]. The cell body, or soma, is the primary component of the neuron and houses the nucleus, which contains the cell's genetic material, as well as other organelles responsible for protein synthesis and metabolic functions. The majority of cellular organelles are synthesized within the cell body and subsequently transported along the axon to locations such as the axon terminal and back to the cell body.

Dendrites are tree-like structures that extend from the cell body and serve to receive incoming signals from other neurons or sensory receptors, transmitting this information to the cell body. In addition to dendrites, a long tubular axon extends from the cell body and is responsible for transmitting information in the form of an electrical pulse known as an Action Potential (AP). A single axon can form connections with multiple neurons via its axon terminals. These connections between neurons are referred to as synapses.

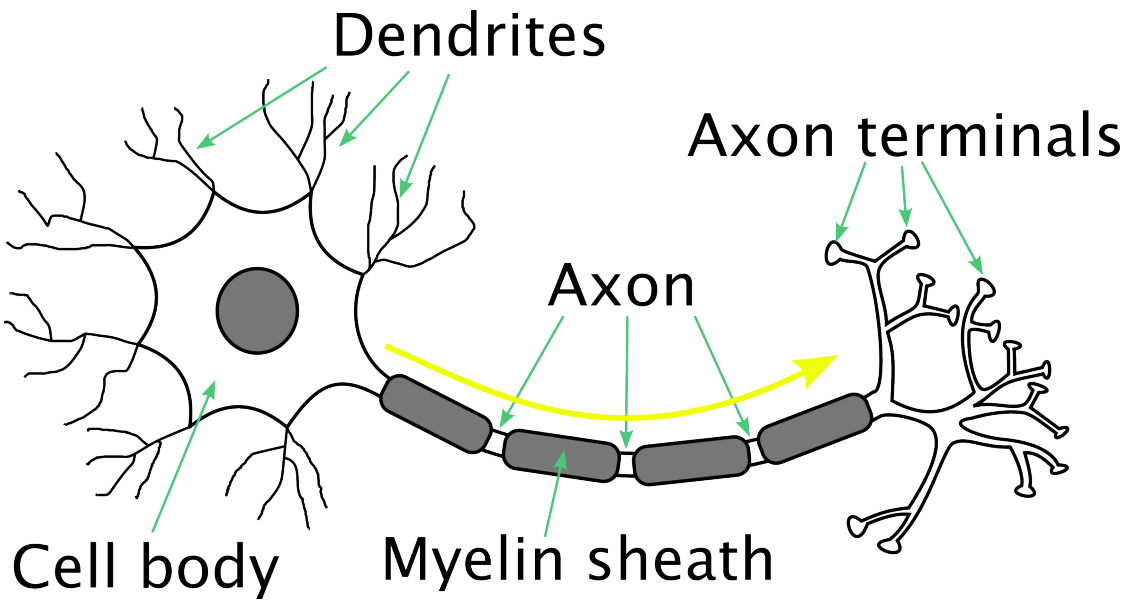

Figure 2.2. **Parts of a neuron** – The propagation of the Action Potential is presented with the yellow arrow.

In chemical synapses, when an AP arrives at the axon terminal, neurotransmitters are released in the direction of the connected cell's dendrite. These neurotransmitters are stored in vesicles and are released via exocytosis due to an increase in Ca^{2+} concentration. The neurotransmitters reach the dendrite of the adjacent neuron within 0.5-1 ms. The propagation of APs can be facilitated by myelin sheaths, which serve to insulate and shield the axon.

2.1.1.2 Electrical Activity of a Neuron

An inactive neuron exhibits a resting membrane potential, which represents the electrical potential difference across the cell membrane when the neuron is not transmitting a signal [2]. At rest, the interior of the neuron is negatively charged relative to the exterior, with a resting potential of approximately -70 mV. This negative charge arises from the unequal distribution of Na^+ and K^+ ions, which is maintained by the active operation of Na^+, K^+ ion pumps within the cell membrane.

The post-synaptic membrane on dendrites contains ligand-binding ion channels that can be activated by neurotransmitters to alter membrane permeability. In the event of Na^+ influx, the interior of the neuron becomes positively charged, resulting in depolarization. Conversely, an increase in K^+ concentration results in hyperpolarization of the cell. These events are classified as sub-threshold post-synaptic membrane potential fluctuations. The dendrites of a neuron accumulate these fluctuations, and when their sum

10.15774/PPKE.ITK.2024.001

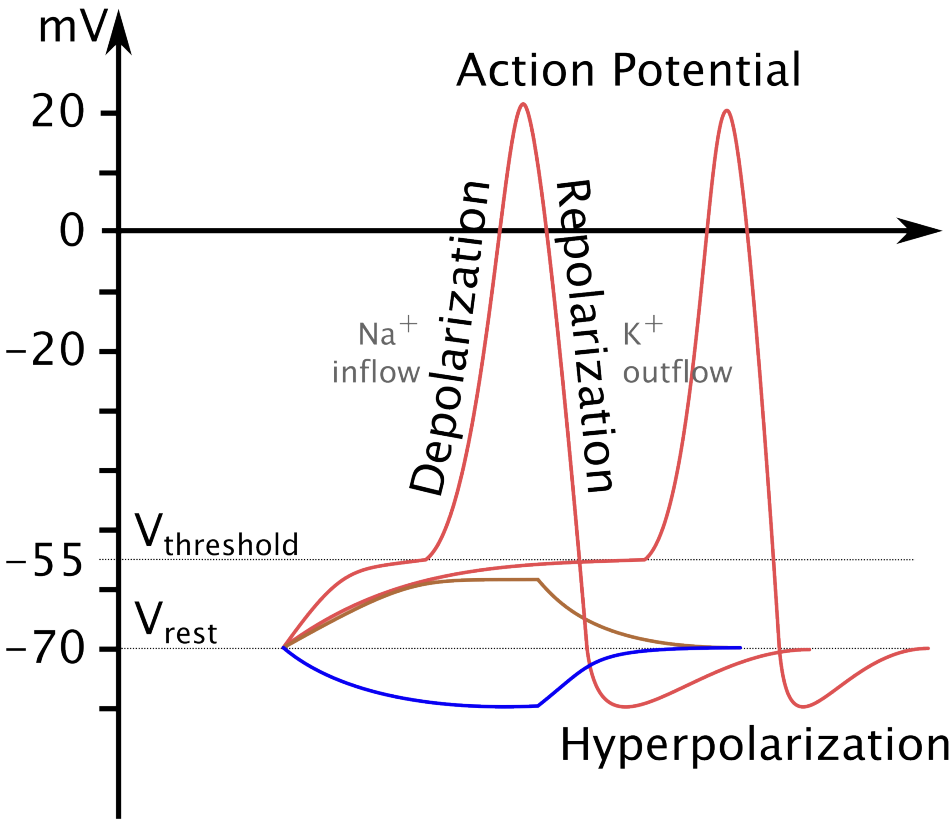

Figure 2.3. **Electrical activity of a neuron** [2] – The resting potential of a neuron is approximately -70 mV. When the spatial and temporal summation of electrical fluctuations on the dendrites reaches the threshold of -55 mV, an Action Potential (AP) is generated at the initial segment of the axon. This triggers the opening of Na^+ channels, allowing Na^+ ions to enter the cell and causing depolarization. Subsequently, when Na^+ channels close, K^+ channels open, inducing repolarization of the cell. After the cell has returned to its resting state, K^+ channels remain open, resulting in hyperpolarization. The resting state is reestablished through active ion exchange between the intra- and extracellular surfaces of the membrane.

reaches the threshold of approximately -55 mV, voltage-gated Na^+ channels in the axon hillock open, permitting Na^+ ions to enter the cell and causing rapid depolarization of the membrane potential. This is followed by the opening of voltage-gated K^+ channels, which induces repolarization of the cell membrane. The K^+ channels close with a slight delay relative to the Na^+ channels, resulting in hyperpolarization of the cell. Following deactivation of the ion channels, active pumps restore the resting state. This fluctuation propagates from the axon hillock to the axon terminals and is referred to as an Action Potential (AP), as depicted in Figure 2.3. An AP is an all-or-nothing signal that propagates without loss along the axon at speeds ranging from 0.1-100 m/s depending on axon diameter and insulation. However, it rapidly dissipates in extracellular space. In contrast, post-synaptic membrane potentials are summed spatially and temporally and propagate over distances in extracellular space.

2.1.2 Invasive Signal Recording Techniques

Various electrodes and techniques have been developed to measure the electrical activity of neurons within the Central Nervous System, as depicted in Figure 2.4. In the context of invasive procedures, microelectrodes are surgically implanted beneath the epidermal layer [2]. The primary target for such implantation is the brain, although implants may also be placed within peripheral nerve fibers or muscle tissue. A key advantage of invasive systems is their ability to capture high-amplitude, low-noise signals. However, issues related to biocompatibility must be addressed.

The material composition of the electrode's tissue-contacting surface is of critical importance, as metallic electrodes may corrode and release toxic substances upon dissolution within the organism. To mitigate such complications, pointed metallic or carbon fiber electrodes are often coated with an insulating layer of lacquer or glass. An additional risk arises from wires and connectors that extend beyond the scalp, as these sites may be susceptible to infection. Furthermore, implanted electrodes may induce neuronal degradation. As a result, the practical application of invasive electrodes is typically restricted to laboratory settings, epilepsy detection and neurosurgery [3], and deep brain stimulation in Parkinson's disease [4].

2.1.2.1 Intracellular Recording

Intracellular measurements involve the measurement of cellular activity within the internal space of a cell, yielding data that closely reflects the actual activity of the neuron,

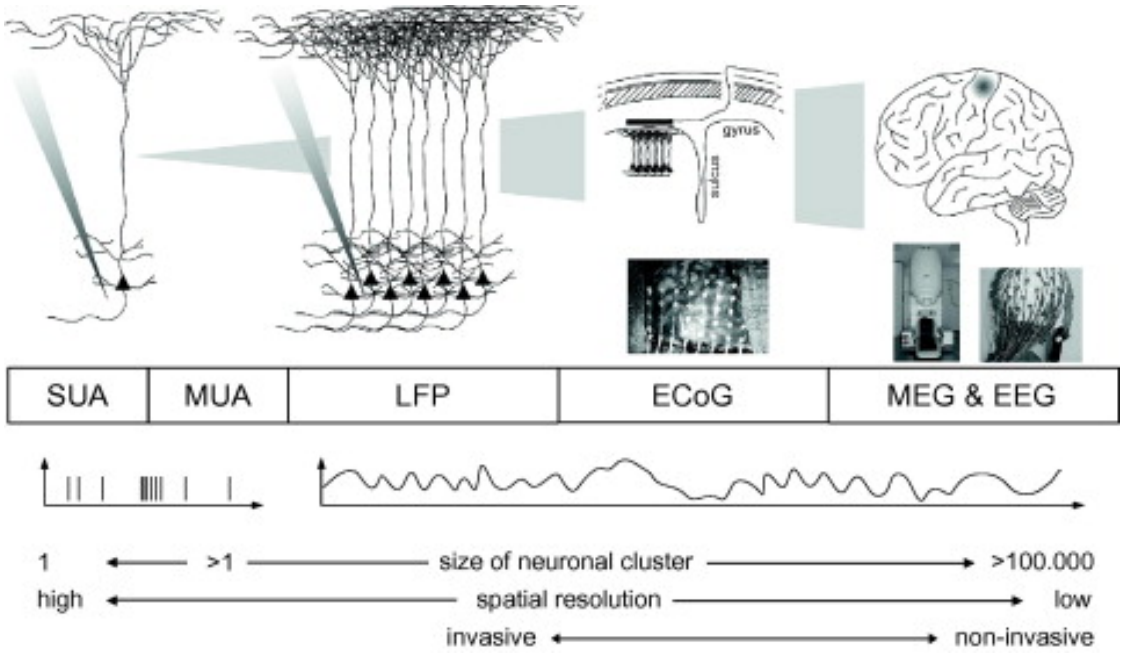

Figure 2.4. Electrophysiological techniques to measure the activity of neurons or regions of the Central Nervous System. [5]

referred to as Single Unit Activity (SUA) [2]. This recording technique is technically complex and is primarily employed in immobilized animals. However, the signal amplitude obtained through this method is high, ranging from 1 to 100 mV.

One implementation of this recording technique involves the insertion of a "sharp" electrode into the perikaryon of a neuron. The body of this electrode is composed of glass to minimize the risk of infection and prevent cell degradation. While the electrode exhibits high resistance and leakage current, it can be deeply implanted. Sharp electrodes facilitate the unambiguous detection of APs.

An alternative intracellular investigative approach involves the use of patch-clamp electrodes. In this technique, the cell is sucked onto the end of the electrode for examination. Due to the high insulation resistance, leakage current is minimal with this method. However, it is typically employed under in vitro conditions, as the electrode head can only access surface cells.

2.1.2.2 Extracellular Recording

Extracellular recording involves the placement of an electrode outside of a cell, enabling the detection of the activity of either single units or multiple neurons, referred to as Multi Unit Activity (MUA) [2]. Electrodes used for this purpose may be constructed from glass capillaries or metal. However, the identification of individual cell action potentials is

not always straightforward for several reasons. Firstly, the extracellular space acts as a strong electrical conductor, resulting in the rapid dispersion of currents. Secondly, the proximity of multiple neurons to the electrode can make it difficult to distinguish the electrical activity of individual cells. Nonetheless, by employing a tetrode, it is possible to infer the activity of individual neurons by analyzing the potential differences recorded on each electrode.

2.1.2.3 Local Field Potential

As one moves away from individual neurons, the amplitude of action potentials decreases exponentially [2]. However, subthreshold membrane potential changes, also known as postsynaptic potential changes, propagate spatially, allowing for the detection of their spatiotemporal summation in analog form using electrodes. This property is referred to as Local Field Potential (LFP). Michigan and Utah electrodes essentially detect a combination of MUA and LFP signals.

To discriminate between SUA, MUA, and LFP signals, spike sorting techniques must be employed following high-pass filtering of raw input above 300 Hz [5], [6]. MUA signals can be obtained by simply applying the same high-pass filter. Pure postsynaptic membrane potential changes can be accessed by implementing a low-pass filter set below 300 Hz.

2.1.2.4 Electrocorticography

Electrocorticography (ECoG) involves the placement of a grid of electrodes directly on the surface of the brain to record its electrical activity [3], [6]. While the amplitude of the signals detected is lower than that of LFP, ECoG offers higher temporal and spatial resolution than Electroencephalography, with a superior signal-to-noise ratio. Furthermore, this method is less susceptible to artifacts such as eye blinks, eye movements, and facial expressions. However, it should be noted that this technique is still considered invasive. In human experiments utilizing ECoG, mu, beta, and gamma waves have been analyzed, which are known to be generated during specific motor activities.

2.1.3 Non-Invasive Signal Recording Techniques

Non-invasive methods for BCIs do not require surgical intervention, simplifying their development, deployment, and use while enabling long-term investigations beyond laboratory settings. However, the resolution of brain bioelectrical signals decreases significantly

with distance from the brain, reducing the signal-to-noise ratio. In contrast, invasive methods such as ECoG provide enhanced degrees of freedom that can be leveraged for control purposes. Nonetheless, the disparity between the methods can be mitigated through advanced signal acquisition and analytical techniques.

2.1.3.1 Magnetoencephalography

Magnetoencephalography (MEG) involves the detection of brain electrical activity by measuring changes in the magnetic field [2]. The source of these signals is the action potential (AP) of neurons, which generates a magnetic field orthogonal to the electric field in accordance with Maxwell's equations. The strength of these signals is in the femtoTesla range (approximately 10-13 T), necessitating the use of a superconducting quantum interference device to capture and convert the signals into voltage changes. These devices are connected to either a flux transformer or superconducting coils, which are placed in close proximity to the subject's head. Due to the size of the complete MEG device and the requirement for a shielded room, it is not suitable for general-purpose BCIs.

2.1.3.2 Electroencephalography

During an electroencephalography (EEG) examination, flat silver-silver chloride electrodes are placed on a person's scalp to measure the summation of subthreshold membrane potential changes appearing on neurons' dendrites [2]. To achieve an acceptable electrode impedance of 5 kΩ, a special gel is applied between the skin and electrode. In cases where a high number of electrodes (> 10) are used, they are fixed in an electrode grid or elastic electrode cap, rather than using adhesive, collodion glue or rubber bands.

EEG is a relatively simple procedure that does not require medical intervention. However, EEG signals have a strength in the microvolt range, resulting in poor signal-to-noise ratios. This is due to signals having to penetrate multiple insulating media (skull, scalp, hair), which distort and decrease their amplitude. Additional factors such as bodily functions or environmental electric noise can also interfere with signals, which are discussed in detail in section 2.3.

2.2. Signals for BCI Control

2.2.1 Electroencephalograms

Electroencephalograms are signals measured during EEG signal acquisition [7]. These signals are categorized according to their frequency range, as presented in Table 2.1.

Table 2.1. Electroencephalograms [2]

EEG bands	**Frequency range (Hz)**
Delta	1 – 4 Hz
Theta	4 – 8 Hz
Alpha	8 – 14 Hz
Beta	14 – 30 Hz
Gamma	above 30 Hz
Slow oscillation & DC shift	below 1 Hz

2.2.1.1 Delta band

The Delta band, located below 4 Hz, is primarily associated with the sleep process [2]. While easily detectable in infants, it disappears in awake adults and can only be detected during deep sleep stages. As such, this band is not suitable for use as a control signal in BCI systems.

2.2.1.2 Theta band

Theta waves, present in the frequency range of 4-8 Hz, are found in small quantities in awake individuals [2], [6]. Similar to delta waves, their presence decreases with age. The amplitude of this band increases during meditation, mental processes, or in situations which involves high emotional states. The theta frequency band is commonly utilized in conjunction with other signals for controlling a BCI system [8], [9].

2.2.1.3 Alpha band

The alpha wave is defined as an EEG signal with a frequency range between 8 and 13 Hz [2], [6]. However, several subcategories of alpha waves have been identified depending on the location of their generation. Specifically, alpha waves detectable above the visual

cortex of the brain are termed alpha waves. The amplitude of this signal increases when the subject is lying in a quiet and relaxed state with eyes closed, avoiding any form of cognitive or physical activity. Another type of alpha range, called the Mu wave, can be detected over the somatosensory and motor cortex and its amplitude modulation is related to movement and motor planning. The Mu wave can be utilized as a control signal in BCI systems, as users can be trained to intentionally generate this signal.

2.2.1.4 Beta band

Beta waves are a type of EEG activity with a frequency range of 14 to 30 Hz that are modulated by voluntary and imagined movements, similar to Mu waves [2], [6]. They are primarily detected over the frontal and central regions of the brain. The appearance of beta waves is associated with the desynchronization of alpha and mu waves. Therefore, in BCI applications, the presence of beta waves is typically examined alongside mu waves during imagined movement paradigms [1].

2.2.1.5 Gamma band

It has been demonstrated that gamma waves, which belong to the frequency range above 30 Hz, are correlated with maximal muscle contractions [2], [6]. When muscle contractions are weak, beta waves replace their presence. In BCI systems, gamma waves are less commonly utilized as they are suppressed as artifacts by Electrooculography or Electromyography signals. It has been also presented in [10], [11] that the skull, skin and hair acts as a lowpass filter, which significantly reduces high frequency components of the EEG.

2.2.2 Event-Related Potentials

Event-related potentials (ERPs) are specialized bioelectrical oscillations consisting of multiple waves that arise in response to external or internal stimuli within a specific time interval relative to the triggering event [2], [7].

2.2.2.1 Slow Cortical Potentials

Slow Cortical Potentials (SCP) refer to the positive or negative shift in EEG signals [1]. This phenomenon is associated with cortical activity and has a latency period ranging from 0.5 to 10 seconds. An increase in cortical function or movement is associated with a negative shift, whereas a positive shift indicates a decrease in neuronal activity [6]. In

an SCP-based BCI system, users must undergo several months of training to produce positive and negative potential shifts.

2.2.2.2 Visual Evoked Potentials

Accoring to Bin et al. [12] the Visual Evoked Potentials (VEPs) refer to ERP signals detected through EEG above the visual cortex which corresponds to the visual information process. VEPs are classified into different groups based on their processing.

In the case of time-modulated VEPs (t-VEPs), non-overlapping signals at a frequency of 4 Hz or less are used for stimulation, and EEG signals are synchronized with the flashing stimuli during recording. The resulting signals are averaged to produce the desired waveform.

In the case of frequency-modulated VEPs (f-VEPs), signals are examined in the frequency domain. Signal processing can be performed through averaging or by analyzing the power spectrum of a longer EEG signal sequence in the frequency domain. When a monitor is used for generating stimuli, the frequency of the flashing stimuli must be an integer divisor of the monitor's refresh rate, otherwise glitching would occur, due to the asynchronization between the stimulus presenter monitor and the actual stimulus.

In code-modulated VEPs (c-VEPs), EEG patterns are paired with pseudorandom sequences of flashing stimuli. This type of modulation is capable of maximizing the amount of generated information under a minute. The use of VEPs does not require any preparation from the user.

2.2.2.3 P300

The P300 component is an ERP wave that reflects the degree of mental attention focused on a specific task [6], [13], [14]. It appears as a positive deflection in the EEG signal over the parietal and central regions of the brain approximately 300 ms after the presentation of a relevant stimulus. The timing of its occurrence is influenced by task difficulty level. To obtain the P300 waveform using the averaging method, the EEG signal must be synchronized with the stimulus that elicits the component. P300 can be elicited by visual or auditory stimuli. When using P300-based BCI, no special preparation is required from the user. However, due to inter-individual variability in P300 waveforms, the system must be trained to recognize the current user's P300 characteristics.

2.2.2.4 Sensory Motor Rhythm

Sensory motor rhythm (SMR) investigates the modulation of Mu and Beta brain waves, which are linked to amplitude modulation of brain activity required for movement [6], [7]. Actual movement execution is not a prerequisite for SMR generation; mere imagination of a given action suffices. Event-related desynchronization can be observed in Mu wave over motor cortex during execution of movement tasks. During this time, Mu band amplitude decreases, beginning approximately 2 seconds before actual movement such as finger movement. A few seconds after movement, Mu band returns to its original level. Beta wave shows desynchronized state at beginning of movement followed by significant synchronization indicating completion of movement execution. In addition to Mu and Beta waves, it may be worthwhile to investigate Gamma band as brief period of synchronization can be observed in this band immediately before movement.

Training is necessary for using an SMR-based BCI system, but this process takes less time than in the case of SCP [1].

2.3. Artifact Filtering

Non-invasively recorded EEG signals have small amplitude, making them susceptible to distortion by electric devices and physiological phenomena [2].

In cases where the EEG system exhibits high impedance between the skin and electrodes, 50 Hz powerline noise may appear on the system. Additionally, radio communications such as mobile, Wi-Fi, and TV generate transient electromagnetic noise, which may manifest as artifacts. The impedance of electrodes can be reduced by using EEG gel or ionized water. Furthermore, a notch filter can be applied to recorded signals.

Electrode movements can generate artifacts with high amplitude and deviation, which may be caused by insufficient fixing of the electrode system, yawning, chewing, or moving the ears.

Physiological artifacts can also appear alongside EEG signals due to human bodily functions. Due to the imperfect orb shape of the eyes, there is a 50-100 mV potential difference between the retina and cornea [1], [2], [6]. When the eye moves, the direction of this DC potential also shifts, creating polarity artifacts on the frontotemporal region of an EEG montage. These signals are referred to as Electrooculograms (EOG).

Muscle activity and corresponding muscle action potential, known as electromyograms (EMG), are greater by one order of magnitude compared to EEG signals. Additionally,

the frequency range of EMG overlaps with that of EEG signals. Jaw movements and facial expressions may manifest as bursting activity.

2.4. Feature Extraction

The feature extraction component of a BCI system aims to increase the signal-to-noise ratio by amplifiying the user's mental commands from the recorded signal-noise mixture. This requires an algorithm that transforms the raw signal into a new form. This step is crucial, as insufficient features are difficult to classify even for advanced non-linear classifiers such as deep neural networks. The following sections present the four different domains of features.

2.4.1 Time Domain

In the time domain, features are generated in such a way that they retain time information.

2.4.1.1 Hudgins' feature set

Hudgins et al. [15] described a feature set comprising five simple features that do not require high computational capacity. This feature set was originally designed for EMG signal classification, but parts of it have been successfully applied to EEG processing tasks [Au5], [16]–[18]. In the following equations X represents an N long vector which includes data from time-series.

1. The Mean Absolute Value (MAV) can be represented by the following equation:

$$\overline{X} = \frac{1}{N}\sum_{k=1}^{N}|x_k| \tag{2.1}$$

2. The Mean Absolute Value Slope calculates the differences between adjacent MAVs:

$$\Delta\overline{X}_i = \Delta\overline{X}_{i+1} - \overline{X}_i \tag{2.2}$$

3. The Zero Crossing (ZC) calculates the number of times the data crosses zero:

$$ZC = \sum_{k=1}^{N-1}\begin{cases}1, & \text{if } x_k \times x_{k+1} < 0 \text{ and } |x_k - x_{k+1}| > \varepsilon \\ 0, & \text{otherwise}\end{cases} \tag{2.3}$$

where ε is a threshold used to filter out noise.

4. The Slope Sign Changes (SSC) counts the presence of local minima and maxima in the region of three consecutive samples x_{k-1}, x_k, x_{k+1}:

$$\{x_k > x_{k-1} \text{ and } x_k > x_{k+1}\} \text{ or } \{x_k < x_{k-1} \text{ and } x_k < x_{k+1}\} \tag{2.4}$$

   Again, threshold value is applied:

$$|x_k - x_{k+1}| \geq \varepsilon \text{ or } |x_k - x_{k-1}| \geq \varepsilon \tag{2.5}$$

5. Waveform Length (WL) was designed to calculate waveform complexity using the following equation:

$$WL = \sum_{k=1}^{N} |\Delta x_k| = \sum_{k=1}^{N} |x_k - x_{k-1}| \tag{2.6}$$

2.4.1.2 Root Mean Square

The Root Mean Square (RMS) provides information about the amplitude of the signal and is calculated using the following equation:

$$RMS = \sqrt{\frac{1}{N} \sum_{k=1}^{N} x_k^2} \tag{2.7}$$

It has been successfully utilized in [17]–[19].

2.4.2 Spatial Domain

In the spatial domain, the most prevalent method for extracting spatial features is the Common Spatial Pattern (CSP), which seeks to amplify the disparities between two classes of EEG samples while minimizing their similarities [6], [20]. This analysis employs normalized spatial covariance matrices, computed as follows:

$$C = \frac{EE^T}{trace(EE^T)} \tag{2.8}$$

where E represents an EEG window with shape *(number of channels* $\times$ *number of samples)* and $trace(x)$ denotes the sum of x's diagonal elements. With respect to the two classes intended for separation, the composite spatial covariance is defined as:

$$C_c = \overline{C_1} + \overline{C_2} \tag{2.9}$$

where C_n represents the mean of a selected class's normalized spatial covariances. By utilizing eigenvectors and eigenvalues, C_c can be expressed as:

$$C_c = U_c \lambda_c U_c^T \tag{2.10}$$

where U_c is the matrix of eigenvectors and λ_c represents the diagonal matrix form of eigenvalues, which are assumed to be in descending order.

The variances in the space spanned by U_c^T can be equalized through the whitening transformation:

$$P = \sqrt{\lambda_c^{-1}} U_c^T \tag{2.11}$$

resulting in all eigenvalues of PC_cP^T being equal to one. If $\overline{C_1}$ and $\overline{C_2}$ are transformed with P as:

$$S_1 = P\overline{C_1}P^T \text{ and } S_2 = P\overline{C_2}P^T \tag{2.12}$$

then S_1 and S_2 will share common eigenvectors. Therefore, if $S_1 = B\lambda_1 B^T$, then $S_2 = B\lambda_2 B^T$ and $\lambda_1 + \lambda_2 = I$, where I denotes an identity matrix. The sum of two corresponding eigenvalues is an invariant of the whitening matrix B, a fundamental property exploited in multivariate data analysis. Specifically, the eigenvectors associated with B's largest and smallest eigenvalues for S_1 and S_2 are inversely related. This characteristic renders B's eigenvectors a valuable tool for classifying the two distributions. By projecting the whitened EEG onto B's first and last eigenvectors, one can obtain feature vectors that are optimally suited for discriminating between two populations of EEG data in the least squares sense. By utilizing the projection matrix $W = (B^T P)^T$, one can map a trial E to:

$$Z = WE \tag{2.13}$$

where the columns of W^{-1} represents the common spatial patterns, which are time-invariant EEG source distribution vectors.

The original CSP algorithm is sensitive to noise, spatial resolution electrode location; therefore, several improved versions of this algorithm have been introduced, such as regularized CSP (RCSP) [21] or the Filter Bank CSP (FBCSP) [22].

2.4.3 Frequency Domain

In the frequency domain, features are extracted by transforming signals from the time domain to investigate their frequency spectrum.

2.4.3.1 Fourier Transformation

A Fourier transform is required to convert signals to the frequency domain. However, since the signals under examination are discrete-time, the continuous-time formula, $x(f) = \int_{-\infty}^{\infty} x(t)e^{-i\omega t}dt$, is not appropriate. Instead, the discrete-time Fourier transform

$X(\omega) = \sum_{n=-\infty}^{\infty} x[n]e^{-i\omega n}$ is required. Nevertheless, even this is not ideal for signals with limited time duration, as the Fourier transform of a finite-length signal is infinite in duration. The actual solution is the discrete Fourier transform:

$$X[k] = \sum_{n=0}^{N-1} x[n]e^{\frac{-i2\pi kn}{N}}, \quad k = 0, 1, \ldots, N-1 \tag{2.14}$$

implemented via the Fast Fourier Transform (FFT) algorithm.

2.4.3.2 Power Spectral Density

Another powerful algorithm for measuring and analyzing the frequency characteristics of EEG signals is the Power Spectral Density (PSD), which is typically estimated using Welch's method [23], [24]. The data is expressed as:

$$X_k(j) = X(j + kD), \quad j = 0, \ldots, L-1, \quad k = 0, \ldots, K-1 \tag{2.15}$$

where $X_k(j)$ represents an L-length data sample from the N-length $X(j)$ data and D denotes the unit step size between segments. The output periodograms are given by:

$$I_k(f_n) = \frac{L}{U}\left[\frac{1}{L}\sum_{j=0}^{L-1} X_k(j)W(j)e^{\frac{-i2\pi jkn}{L}}\right]^2 \tag{2.16}$$

where $f_n = n/L, \quad n = 0, \ldots, L/2$ and $W(j)$ represents a window. The window function U defines the normalization factor of the power as:

$$U = \frac{1}{L}\sum_{j=0}^{L-1} W^2(j) \tag{2.17}$$

Finally, Welch's PSD is defined as the average of the periodograms:

$$\hat{P}(f_n) = \frac{1}{K}\sum_{k=0}^{K-1} I_k(f_n) \tag{2.18}$$

2.4.4 Time-frequency Domain

Time-frequency domain features endeavor to combine both temporal and spectral information to augment the informational content of the features.

2.4.4.1 Short Time Fourier Transformation

The Short Time Fourier Transformation (STFT), in contrast to the PSD, does not average the Fourier transformed windowed signals [25]–[27]. Rather, it concatenates the segments,

thereby generating a two-dimensional time-frequency spectrogram of the signal. The STFT is mathematically defined as:

$$STFT(\tau, \omega) = \int_{-\infty}^{+\infty} x(t)w(t-\tau)e^{-jwt}dt \tag{2.19}$$

where τ is the window position on the time axis and $w(t)$ represents a window.

2.4.5 Wavelet Transformation

The Wavelet Transform (WT) seeks to expand and enhance the capabilities of the STFT algorithm [6], [24]. In the case of STFT, there exists a trade-off between frequency and temporal resolution. A longer window results in higher frequency resolution; however, this comes at the expense of reduced temporal resolution. The WT was designed to concurrently investigate the time-frequency representation of data through the utilization of modulated windows known as wavelets. These wavelets are modulated by shifting and scaling and matched to the signal along the time axis.

During the continuous wavelet transformation (CWT), the wavelet coefficient is defined as:

$$w(s, \tau) = \int_{-\infty}^{+\infty} x(t)\psi^*_{s,\tau}(t)dt \tag{2.20}$$

where $x(t)$ represents the EEG signal, s is the scale, τ denotes the shifting factor and $\psi_{s,\tau}(t)$ represents the wavelet function, which is complex conjugated and can be calculated as follows:

$$\psi_{s,\tau}(t) = \frac{1}{\sqrt{s}}\psi\left(\frac{t-\tau}{s}\right) \tag{2.21}$$

Here $\psi(t)$ is the mother wavelet. There exist multiple types of mother wavelets (such as Morlet, bi-scaled and Mexican hat), each possessing distinct characteristics. However, all wavelets must satisfy the following condition:

$$\int_{-\infty}^{+\infty} \psi(t)dt = 0 \tag{2.22}$$

The CWT suffers from redundancy due to the continuously changing scaling and shifting parameters; hence this algorithm is both time-consuming and computationally intensive.

The Discrete Wavelet Transformation (DWT) was introduced to address these shortcomings and reduce the complexity of the CWT. It creates a multiscale representation by generating specific numbers of scales from the mother wavelet. In each step from the source signal, a detail and an approximation are generated by using a high pass and a lowpass digital filter respectively. Each generated signal is downsampled by 2 and the approximation can be further processed with the previously described steps.

2.5. Classification

The objective of a classifier is to differentiate between obtained features based on their inherent properties. A multitude of machine learning algorithms can be utilized for this purpose, which segregate distinct classes from one another by establishing a hyperplane. The calibration of the hyperplane responsible for the separation is referred to as learning, during which the algorithm must be provided with the class label for each input feature. To attain optimal separation, it is recommended to employ data during the training phase that uniformly encompasses the space of the different classes. Once it has been ascertained that adequate separation has been achieved as a consequence of learning, the classifier can be employed in practice, where it responds to input features with probabilities of class membership. The class with the highest probability can be regarded as the outcome.

2.5.1 Linear Discriminant Analysis

Linear Discriminant Analysis (LDA) [6] is one of the most elementary classification algorithms with minimal computational requirements, rendering it a popular choice in BCI applications. In the binary case, it is assumed that the classes can be segregated with a linear hyperplane in the feature space, which is mathematically defined as:

$$g(\mathbf{x}) = \mathbf{w}^T\mathbf{x} + b \tag{2.23}$$

where $\mathbf{x}$ represents the input feature, b is the bias term and w denotes the weight vector. For an input $\mathbf{x}$, the class label is assigned according to $sign(g(\mathbf{x}))$. The $\mathbf{w}$ projection vector can be estimated as follows:

$$\mathbf{w} = \Sigma_c^{-1}(\mu_2 - \mu_1) \tag{2.24}$$

where μ_i is the calculated mean of class i and the Σ_c represents the common covariance matrix which is defined as $\Sigma_c = \frac{1}{2}(\Sigma_1 + \Sigma_2)$. The mean and the covariance matrix are estimated as:

$$\mu = \frac{1}{n}\sum_{j=1}^{n}\mathbf{x}_j \tag{2.25}$$

$$\Sigma = \frac{1}{n-1}\sum_{j=1}^{n}(\mathbf{x}_j - \mu)(\mathbf{x}_j - \mu)^T \tag{2.26}$$

where the $\mathbf{x}$ matrixes are containing n feature vectors $\mathbf{x}_1, \mathbf{x}_2, \ldots, \mathbf{x}_n \in \mathbb{R}^d$. To enhance the accuracy of LDA, several modified versions of the algorithm have been published. The shrinkage LDA introduced a novel estimation formula for the covariance matrix:

$$\Sigma = (1-\gamma)\Sigma + \gamma v I \tag{2.27}$$

where the γ shrinkage parameter is tunable and controls the amount of regularization. This parameter can be set between 0 and 1. The v parameter is expressed as $trace(\Sigma)/d$, where d denotes the dimensionality of the feature space.

2.5.2 Support Vector Machine

The original Support Vector Machine (SVM) problem was formulated by Vapnik [28]. Given a training set $(\mathbf{x}_i, y_i)$, $i = 1, \ldots, k$ where $\mathbf{x}_i \in \mathbb{R}^n$ represents a training sample with label $y_i \in \{-1, 1\}$, the SVM solves the following optimization problem:

$$\min_{\mathbf{w},b,\xi} \frac{1}{2}\mathbf{w}^T\mathbf{w} + C\sum_{i=1}^{k}\xi_i \tag{2.28}$$

subject to

$$y_i(\mathbf{w}^T\phi(\mathbf{x}_i) + b) \geq 1 - \xi_i, \quad \xi_i \geq 0 \tag{2.29}$$

where ϕ denotes a nonlinear function that can maps $\mathbf{x}_i$ to a higher-dimensional feature space, $\mathbf{w}$ is the weight vector, b is the bias, and $C > 0$ represents a penalty hyperparameter of the error term. The term $K(\mathbf{x}_i, \mathbf{x}_j) \equiv \phi(\mathbf{x}_i)^T\phi(\mathbf{x}_j)$ is referred to as the kernel function and can be an arbitrary mathematical equation. The most used kernel functions are as follows:

- Linear: $K(\mathbf{x}_i, \mathbf{x}_j) = \mathbf{x}_i^T\mathbf{x}_j$
- Polynomial: $K(\mathbf{x}_i, \mathbf{x}_j) = (\gamma\mathbf{x}_i^T\mathbf{x}_j + r)^d, \quad \gamma > 0$
- Radial-Basis-Function (RBF): $K(\mathbf{x}_i, \mathbf{x}_j) = exp(-\gamma\|\mathbf{x}_i - \mathbf{x}_j\|^2), \quad \gamma > 0$

where γ, r, and d denote the kernel parameters that can also be considered hyperparameters.

This algorithm aims to maximize the margin of the hyperplane between feature vectors of the training sample that are in closest proximity to the plane. These data points are also referred to as support vectors. The kernel function projects the feature set into a higher-dimensional space in order to identify the most optimal hyperplane.

2.5.3 Artificial Neural Networks

Goodfellow described Deep Learning [29] as an application of artificial intelligence that solves complex problems, the results of which are influenced by many factors. This method can learn high-level features by solving and combining multiple simple representation problems. Deep Learning is achieved through an Artificial Neural Network (ANN) with multiple hidden layers.

According to Haykin's Neural Networks and Learning Machines book [30], the fundamental unit of an ANN is the perceptron, which aims to emulate the information processing behavior of a biological neuron. A perceptron possesses multiple input lines, analogous to the dendrites of a biological neuron, which collects and weights the input data before generating an output through a non-linear function. A perceptron can classify linearly separable data into two classes. The classification is mathematically defined by the following equation:

$$y(n) = \phi(\mathbf{w}^T(n)\mathbf{x}(n)) \tag{2.30}$$

where $\mathbf{w}$ denotes the weight vector with $\mathbf{w}_0 = b$ bias, $\mathbf{x}$ is the input vector with $\mathbf{x}_0 = 1$, and ϕ represents the non-linearity function which generates the y output. The perceptron model is presented in Figure 2.5. The weight of the perceptron can be trained to accurately classify data from two given classes using the weight adaptation equation:

$$\mathbf{w}(n+1) = \mathbf{w}(n) + \eta(d(n) - y(n))\mathbf{x}(n) \tag{2.31}$$

where n is the timestep, $\eta > 0$ represents the learning rate and $d(n)$ denotes the required response [30].

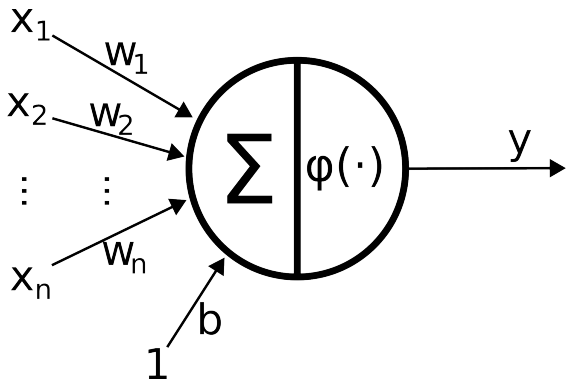

Figure 2.5. Perceptron, where $\mathbf{x}_k$ is the input, $\mathbf{w}_k$ is the weight, b is the bias, Σ is the combination of the weighted input signals and ϕ is the nonlinearity, which generates the y output [30].

If a problem is not linearly separable, multiple perceptrons can be employed to construct an ANN, where several perceptrons are organized into multiple layers. An example is depicted in Figure 2.6. The increasing number of layers and perceptrons can increase the complexity of the network and hyperplane. However, more parameters necessitate greater computational capacity and training data. ANNs are trained through backpropagation as follows: First, the input signal is propagated from the input layer to the output layer while keeping the weights of the network fixed. Second, at the output, the error

signal is calculated and propagated back from the output to the input. This signal is utilized to update the weights of the ANN.

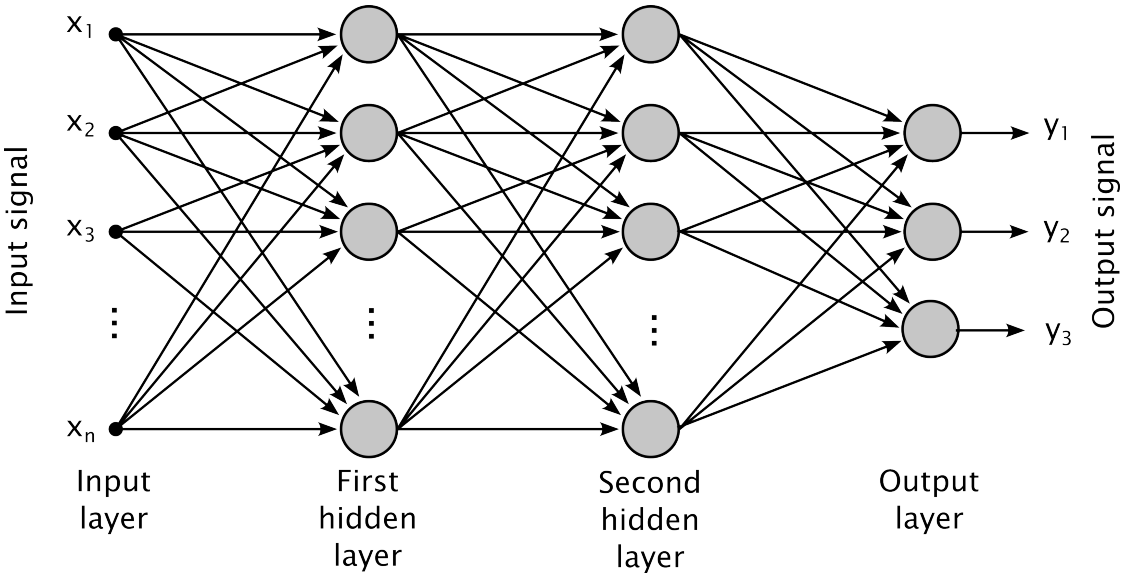

Figure 2.6. Feed Forward Neural Network with two hidden layers [30]

Convolutional Neural Networks (CNNs) are specialized multi-layered perceptrons designed to classify patterns specifically on image-like inputs. CNNs employ a kernel matrix that aims to extract local features. Using this kernel, the exact orientation and location of a pattern become less significant while relative connections become more important. Generally, a convolutional layer is succeeded by a subsampling layer that aims to reduce both the number of trainable parameters and network sensitivity. Prior to outputting results, feature maps are flattened and followed by several layers of fully connected perceptrons. The fully connected output layer is responsible for generating probabilistic output by utilizing the softmax function. An example representation of a network is presented in Figure 2.7.

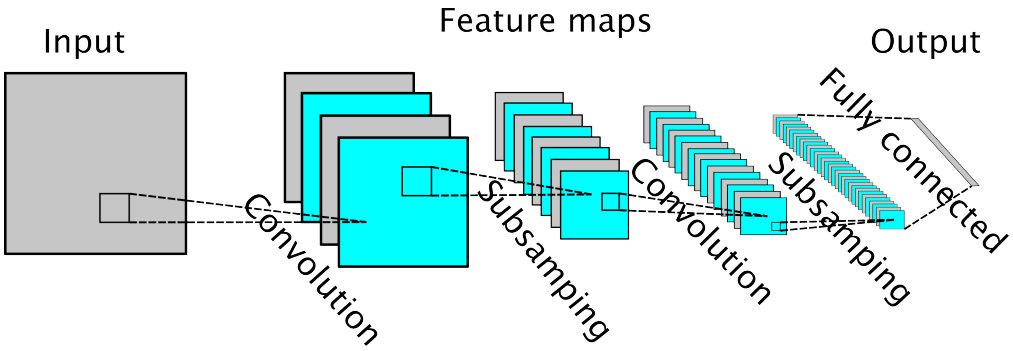

Figure 2.7. Example structure of a Convolutional Neural Network [30]

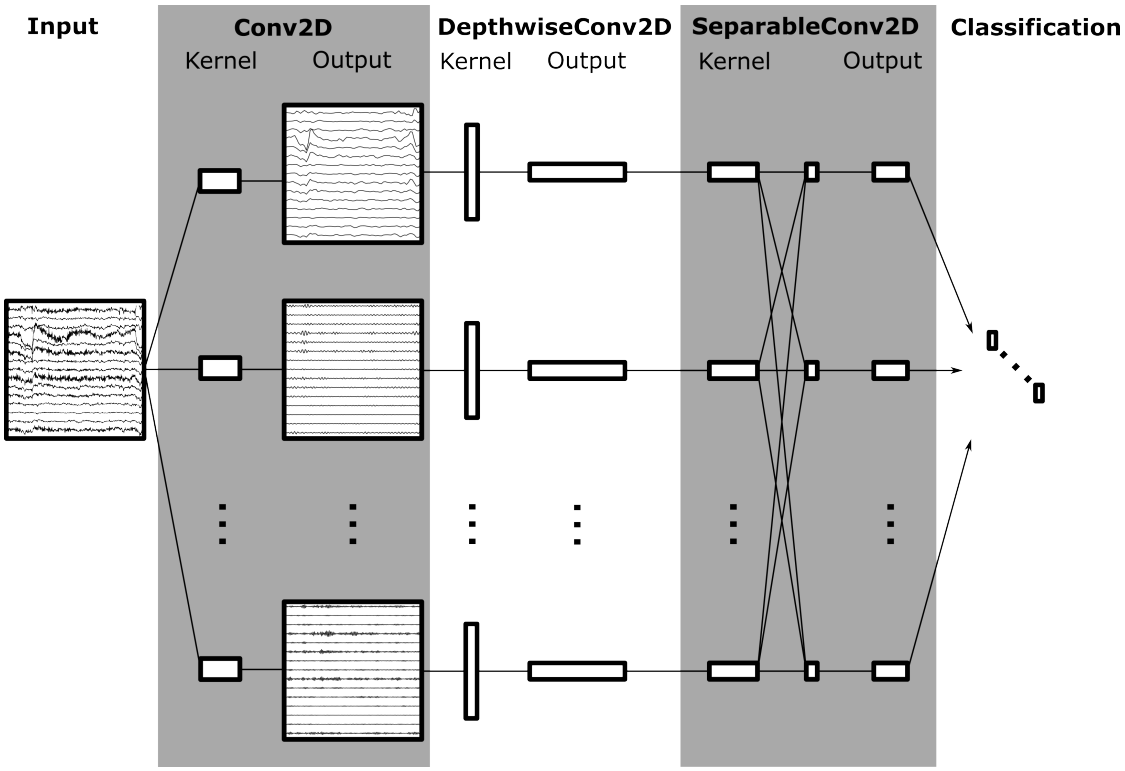

Figure 2.8. EEGNet architecture [31]

The EEGNet [31] was the first CNN designed to utilize and learn the frequency, spatial, and temporal information of the Electroencephalography (EEG) signal simultaneously. It was also designed for multiple EEG paradigms. The complete architecture is presented in Figure 2.8. The temporal convolutions of the network extract frequency information as frequency filters. This is followed by a depthwise convolution block, which learns the spatial information from the frequency filtered data. As a final step, separable convolution was utilized with aims to learn the temporal summary of the previously extracted features individually, which was followed by a pointwise convolutional block to produce an optimal mixture of the resulted feature maps. This state-of-the-art network started a new trend, to optimize CNN architectures for EEG singal classification, which is further discussed in Chapter 4.

2.6. First types of BCI systems

In this section the first successfully implemented BCI systems are presented, which utilize the previously described electrophysiological phenomena.

2.6.1 SCP-based BCI

In the 1990s, Birbaumer and colleagues successfully demonstrated that individuals with late-stage ALS could learn to control their SMR to operate a binary-choice communication system [1]. The BCI provided users with the first half of the alphabet and allowed them to indicate whether their target letter was present or not. Subsequent steps involved progressively halving the selected group until the desired letter was obtained. A major disadvantage of this method is the speed: only 0.15-3.0 letters can be described with it per minute.

2.6.2 VEP-based BCI

In the 1970s, Jacques Vidal developed a VEP-based system for controlling a computer cursor by tracking the user's gaze direction [1]. The system utilized VEP signals to determine the direction of the user's gaze and moved the cursor accordingly. In 1992, Shutter and colleagues created a novel BCI device that displayed an 8x8 character matrix and elicited VEPs through flickering it. The user had to focus their gaze on the character they wished to select. With this BCI system, healthy individuals were typically able to generate 10-12 words per minute.

2.6.3 P300-based BCI

Donchin and Farwell [32] are credited with creating the first computer typing program based on the P300 component. The implementation of the BCI system utilized the Oddball paradigm, where the user is required to distinguish rare stimuli from standard ones. In the auditory domain, this can be achieved by presenting short, high-pitched beeps of two different frequencies, where the rare signal replaces the standard one with a given probability. Users are instructed to count the rare signals to maintain attention. Building on this paradigm, Donchin and colleagues developed a 6x6 character matrix that randomly flashed rows and columns, with users instructed to count the flashes corresponding to their target character. The system determined the selected character by finding the intersection of the row and column with the highest P300 response. Generating a P300

response requires signal averaging, emphasizing the need to synchronize EEG signals with evoking stimuli.

2.6.4 SMR-based BCI

Wolpaw et al. [33] successfully implemented cursor control in a limited vertical direction on a computer using the mu brain wave. The user was required to consistently navigate the cursor into a square displayed on the top or bottom of the screen, which was accomplished through the alteration of their mu rhythm amplitude. The direction of the cursor movement was correlated with the amplitude of the signal. High amplitude mu rhythm made the cursor to move up and low amplitude to move it down.

Working with colleagues, Pfurtscheller differentiated simple movements from one another by separating SMRs associated with hand and foot movements on both left and right sides [1]. As a result, they were able to control a cursor and wheelchair as well as select letters or other symbols.

Leeb et al. [34] presented both robotic control and speller applications. In the former case, users had to control a robot through a real office-like environment and reach target areas; in the latter task, users had to write predefined words using the so-called BrainTree program. In both cases, PSD of mu and beta waves were calculated concerning event-related synchronization and desynchronization; decisions were obtained using a Gaussian classifier.

10.15774/PPKE.ITK.2024.001

Chapter 3

Proposed Closed Loop BCI System for Cybathlon 2020

3.1. Introduction

The Cybathlon Competition was first introduced on October 5th, 2014 [35]. This event, also known as the "Bionic Olympics", provides a platform for research groups, industrial companies, and technology providers to showcase their products, applications, and technologies across six disciplines with the assistance of physically disabled subjects, referred to as pilots in Cybathlon terminology. The six disciplines include Brain-Computer Interfaces, Functional Electrical Stimulation Bike Race, Leg Prosthesis, Powered Arm Prosthesis, Powered Exoskeleton, and Powered Wheelchair.

In the BCI discipline of Cybathlon, pilots with quadriplegia compete in a car-racing-like computer game by controlling their avatar using well-timed imagined mental commands recorded by EEG. The raw EEG data recorded is often subject to internal or external noise interference such as eye blinking, swallowing, electric powerline noise or motion artifacts. The use of any artifact for control is strictly prohibited and the implementation of a filtering and artifact rejection algorithm is mandatory. The computer game can be controlled using three active commands plus the absence of any commands. Pilots are required to reach the finish line within 240 seconds.

Perdikis et al. [36] participated in the first Cybathlon competition with two pilots forming a team called Brain Tweakers. They utilized EOG electrodes and the FORCe algorithm to detect artifacts. Laplacian derivation was performed on pure EEG signals as a special filtering technique, followed by Power Spectral Density calculation on 2 Hz wide frequency intervals. The resulting features were classified using the Gaussian mixture

model. Two class motor imaginary signals were used, namely movements of Both Hands and Both Feet. To meet the requirements for controlling the game, they implemented a strategy where if two different types of commands were generated within a configurable time window, the third active control signal was sent to the game. Instead of further developing and fine-tuning the control algorithm, they focused on training their pilots, asserting that learning to purposefully modulate brain waves significantly impacts the usability of the BCI system. As evidence of their hypothesis, one of their pilots won the Cybathlon 2016 competition and they successfully employed their algorithm in both the Cybathlon BCI Series 2019 and Cybathlon Global Edition 2020 competitions as WHI Team [37], achieving first place.

Team MIRAGE91 from Graz [38] developed an online artifact detection system that included a blinking detector by thresholding on the band power of the AFz electrode and autoregressive modeling to detect high deviations. For feature extraction, they used Common Spatial Pattern with shrinkage regularized Linear Discriminant Analysis for classification at Cybathlon 2016. They implemented a 3-class paradigm with a thresholding strategy using the following motor imagery (MI) tasks: Left Hand, Right Hand, and Both Feet. The control output was only sent to the game if the classification probability met the threshold. Their pilots demonstrated a smooth learning curve; however, they encountered unexpected issues during the competition and performed below their training results. For the Cybathlon BCI Series 2019 and Cybathlon Global Edition 2020 competitions, they improved their algorithm by incorporating a novel adaptive thresholding algorithm [39] for controlling the output of the BCI.

In parallel with the Cybathlon, numerous efforts have been focused on developing suitable offline BCI systems capable of accurately classifying EEG signals originating from MI tasks [22], [31], [40], [41]. Many of these systems employ artificial neural networks as a classifier [Au2], [Au3], [40], [42]. The EEGNet [31], developed by Lawhern et al., is one of the state-of-the-art networks. One advantage of this algorithm over simpler classification methods is that it does not require any feature-extracted signal; instead, it only requires raw EEG data in matrix form and learns features similar to FBCSP [22]. However, simple classifier methods, such as K-Nearest-Neighbor [43], [44], LDA [43], [45] or SVM [46]–[48] are also preferred in BCI systems, where computational requirements are planned as modest, as in our approach, presented in section 3.2.2 below. Therefore, we selected SVM for our algorithm and compared it with the state-of-the-art EEGNet. The majority of classifier comparison studies utilize one of the BCI Competition datasets

[49]–[52]; however, these datasets contain only a limited number of subjects (≤ 10). In [42], [44], [53] the MI dataset on PhysioNet [54] is utilized. This database was created with the participation of 109 subjects; therefore, we selected it for comparison to ensure statistical significance.

The following sections aims to present the comprehensive development trajectory of a BCI system, designed for the Cybathlon Global Edition 2020 by the Hungarian research team, Ebrainers. During the design we aimed to generate a subject-specific BCI pipeline instead of a general one, as it was reported in [31], [55], to be superior in classification results. The development process commenced with the creation of signal processing and classification algorithms, which were subsequently validated offline using the PhysioNet dataset. Concurrently, we engaged subjects with tetraplegia in recording experiments. Following data evaluation and algorithm optimization, a real-time BCI system was implemented to interface with the video game provided by the Cybathlon 2020 organizers. Regular experimentation continued until March 5^{th}, 2020, when the advent of the pandemic resulted in the cancellation of further experimentation and our participation in Cybathlon 2020.

3.2. Materials and Methods

To create a BCI system, which can be used to control a computer game, the first step is to acquire a reliable database, which includes not even a large amount of EEG signals but also the correct event markers of the experimental tasks with appropriate labels as annotations. Accurate labeling is essential for appropriately testing the precision the later developed feature extraction and classification algorithms.

3.2.1 Physionet Database

The EEG Motor Movement/Imagery Dataset, accessible via PhysioNet (Physionet) [54] at `https://physionet.org/content/eegmmidb/1.0.0/`, represents one of the biggest repositories of MI task-based data, acquired using the BCI2000 system [56]. The Physionet dataset contains EEG recordings from 109 subjects, obtained using a 64-channel 10-20 EEG system.

In summary, the experimental paradigm employed by Physionet entailed the following: At the onset of the experiment, subjects underwent two one-minute baseline sessions, during which they were instructed to remain calm with eyes open and subsequently closed. This was followed by a movement execution and imagination period, during

which subjects were required to perform overt Left Hand and Right Hand movements, succeeded by an imaginary session involving covert movement. Subsequently, executed and imagined sessions involving Both Hands and Both Feet were conducted. These tasks were repeated three times sequentially, resulting in a total of 14 experimental sessions in addition to the two baseline sessions. Each executed and imagined movement lasted for 4 seconds and was followed by a 4-second resting period.

Due to minor data acquisition issues with the Physionet database, we elected to exclude subjects 88, 89, 92, and 100 for the following reasons: In the case of subject 89, we discovered that the labels were incorrect. The records of subjects 88, 92, and 100 deviated from the primary database description. The duration of the task execution and resting phases were altered to 5.125 and 1.375 seconds respectively. Furthermore, a sampling frequency of 128 Hz was employed instead of the original 160 Hz. These issues have been reported in [42], [53].

3.2.2 Signal Processing and Classification

This section delineates the central component of the BCI system, encompassing artifact rejection, feature extraction, and classification methodologies. The comprehensive signal processing architecture is presented in Figure 3.1. The System's source code, developed and implemented in Python, is accessible at: `https://github.com/kolcs/bionic_apps` and utilize state-of-the-art EEG signal processing and machine learning packages such as MNE [57] and TensorFlow [58].

3.2.2.1 Artifact Rejection Algorithm

The Fully Automated Statistical Thresholding algorithm (FASTER), as published by Nolan et al. [59], was employed for the purpose of artifact rejection, with minor modifications as detailed below. András Adolf, my fellow Ph.D. student, created a Python implementation of the algorithm, which was derived from Vliet's work [60]. This algorithm comprises four steps, designed to eliminate channels, epochs, and components where the Z-score of specified parameters exceeds 3. In the first step, EEG channels exhibiting a Z-score exceeding the threshold for variance, correlation, or Hurst exponent are removed. Subsequently, epochs are discarded based on amplitude range, deviation from channel average, and variance parameters. The third step seeks to eliminate artifact-related components of the signal using independent component analysis (ICA), which separates time-dependent data into statistically independent waveforms. The algorithm

produces a mixing matrix that transforms EEG data into Independent Components (ICs) through multiplication. This computation was performed using the FastICA implementation of the Scikit-learn package [61]. ICs are omitted if their correlation is high with designated electrodes closest to the eyes, thereby filtering out blinking artifacts. Additionally, ICs exhibiting a Z-score greater than 3 for kurtosis, power gradient, Hurst exponent, or median gradient are discarded. To transform the ICs back into the time domain, multiplication by the inverse of the mixing matrix is performed. In the fourth step, bad channels within individual epochs are identified based on variance, median gradient, amplitude range, and channel deviation parameters. All channels designated as bad, including those marked in previous steps, are interpolated using spherical spline interpolation. While the original FASTER algorithm [59] comprises five steps, the final step - detecting artifacts across subjects - was omitted to create a subject-specific process.

Although originally designed for offline brain signal processing, our aim was to utilize the algorithm in real-time. Consequently, minor modifications were made to implement an online version of FASTER. The most time-consuming aspect of the original code is the generation of the ICA matrix; as this cannot be performed online, the matrix is computed using a prerecorded training dataset from the Online Paradigm. Globally bad channels are also determined using this training data. The second step of the FASTER algorithm is omitted in our implementation, as all incoming data must be processed during the real-time gameplay. In the third step, the precalculated ICA matrix is used for transformation and online filtering of components. The fourth step remains unchanged in our online version of the algorithm.

3.2.2.2 Feature Extraction

During feature extraction, epochs were generated from the artifact filtered EEG signals with reference to event markers. Each epoch commenced at the event marker and terminated 4 seconds later, corresponding to the duration of MI task execution by experimental subjects. A majority of EEG processing and classification methodologies reported in BCI competition datasets [49]–[52] generate 2-second-long windows from epochs [22], [25], [31], [40], [62], [63]. However, a review of complete BCI systems employed in Cybathlon competitions reveals a preference for 1-second-long windows for real-time signal processing, feedback, and control mechanisms [36]–[38], [64]–[66] to avoid time lag emphasized in [67]. Therefore, shorter 1-second-long EEG windows were extracted from the generated epochs using a sliding window approach with a 0.1-second shift.

10.15774/PPKE.ITK.2024.001

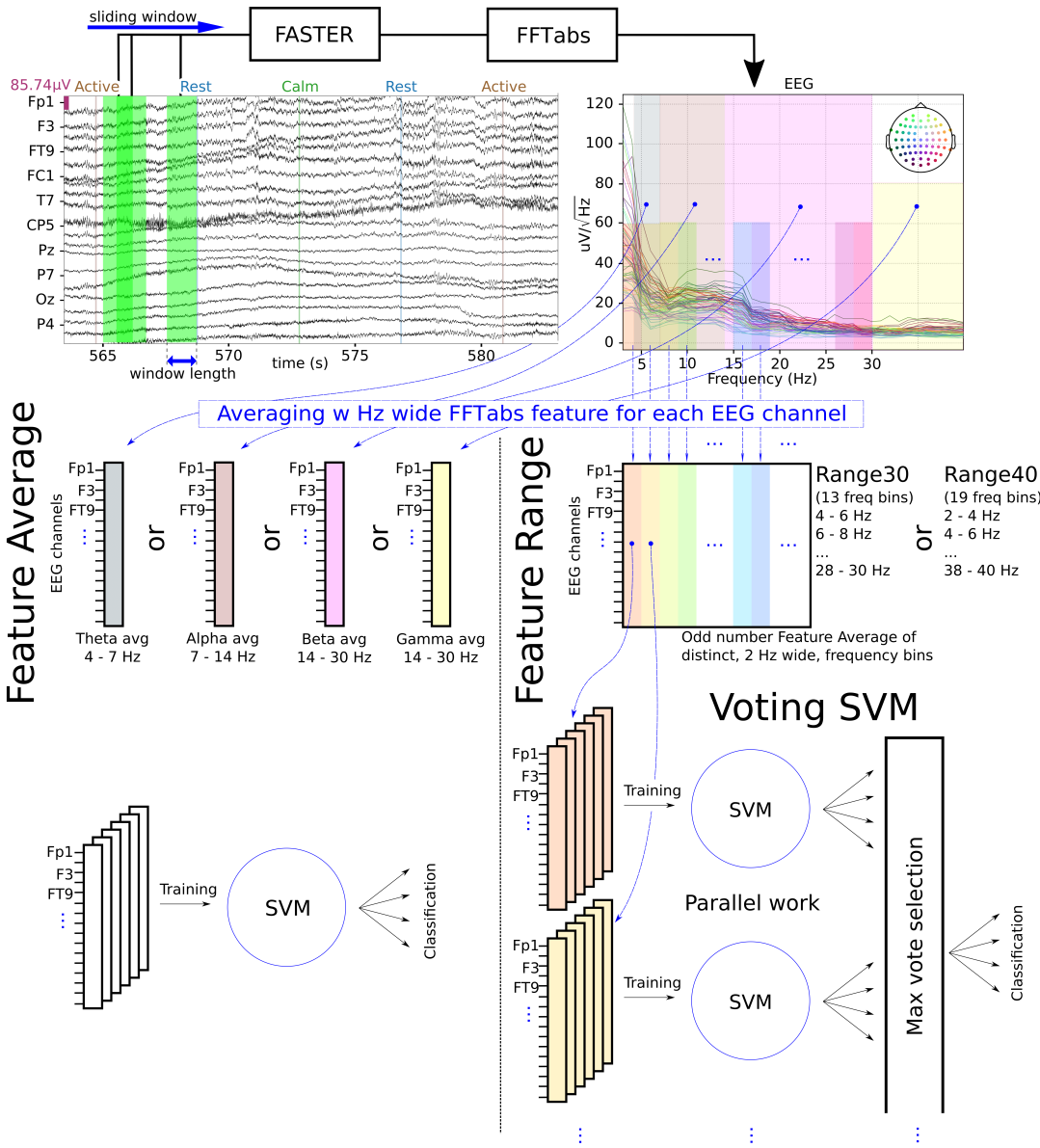

Figure 3.1. **BCI pipeline** – The FASTER algorithm was employed to eliminate EOG and EMG artifacts from raw EEG signals. The absolute value of the Fast Fourier Transformation (FFTabs) was computed as a feature for each EEG channel using a 1-second window. With the Feature Average method, the mean of the FFTabs was calculated for each channel within a specified frequency range, which could correspond to one of the canonical EEG bands (Theta, Alpha, Beta, Gamma). These features were utilized to train a Support Vector Machine (SVM). The Feature Range method builds upon and extends the Feature Average method. The Feature Average was computed for an odd number of distinct frequency bins, each 2 Hz wide. Each feature, corresponding to a frequency bin, was used to train a separate SVM, with the final classification result determined by taking the maximum vote of all SVM units.

Subsequently, the absolute value of the complex Fast Fourier Transformation [68] (FFTabs) was computed for each EEG channel as a frequency domain feature. The FFTabs function was utilized in subsequent methods.

Feature Average In our Feature Average method, the numerical average of FFTabs values was calculated in a specified frequency range for each EEG channel, as represented by the following equation:

$$feature_{ch_i} = \frac{1}{N} \sum_{f=f_{min}}^{f_{max}} \text{FFTabs}_{ch_i}(f) \tag{3.1}$$

where ch_i denotes the i^{th} EEG channel and N represents the number of FFTabs samples in the defined $[f_{min}, f_{max}]$ frequency range.

This process can be interpreted as the truncation of FFTabs to the selected frequency interval and subsequent compression of this matrix into a *channel number* $\times$ 1 feature vector. The boundaries of the frequency range constitute parameters that can be selected to correspond to one of the canonical EEG bands: theta (4-7 Hz), alpha (7-14 Hz), beta (14-30 Hz), and gamma (30-40 Hz).

Feature Range The Feature Range method builds upon and extends the Feature Average. Our objective was to augment the information content of the calculation relative to the Feature Average, analogous to the manner in which the FBCSP [22] sought to improve upon the performance of the original Common Spatial Pattern algorithm. This method generated multiple Feature Averages for non-overlapping, 2 Hz wide frequency bins. This method has two parameters defining the lowest and highest frequency edges. The first frequency bin ranges from f_{low} to $f_{low} + 2Hz$ and the last from $f_{high} - 2Hz$ and f_{high}. We created two feature sets from Feature Range, called range30 and range40, where the numbers correspond to f_{high}. In the case of range30 $f_{low} = 4Hz$ and $f_{high} = 30Hz$, which resulting in a total of 13 frequency bins. Consequently, the size of the feature matrix is *channel number* $\times$ 13. In the case of range40 $f_{low} = 2Hz$ and $f_{high} = 40Hz$, resulting in a total of 19 frequency bins.

3.2.2.3 Feature Normalization

After calculating the features, L2 normalization was performed to enhance classification outcomes, as reported in [69]. The L2 normalization is defined as follows:

$$X_{l2} = X \Big/ \sqrt{\sum_{k=1}^{n} |x_k|^2} \tag{3.2}$$

where X is a n long vector and x_k is the k$^{\text{th}}$ value in the vector.

3.2.2.4 Support-Vector Machine based Classifiers

As a classification tool, we employed the Support Vector Machine (SVM) methodology, owing to its modest computational demands and frequent utilization in BCI applications [46]–[48], [65].

To solve the SVM problem, we utilized the Scikit-learn package [61], which encompasses numerous efficient implementations and other useful machine learning tools. From the available SVM classifiers in Scikit-learn, we selected the SVC class, which defines an RBF-kernelled Support Vector Classifier. The default hyperparameters were employed in all experiments for all classifications. In the case of the Feature Average method, *channel number* $\times$ 1 size feature vectors were used to train and classify data.

In the case of the Feature Range method, feature vectors of frequency bins were used to train separate SVMs in parallel. Consequently, each SVM unit was trained on different EEG bands (e.g., 4-6 Hz and 6-8 Hz) and learned distinct characteristics of brain signals. Each SVM unit made its own classification decision and individual results were aggregated using the majority vote method to compute the final classification result. To avoid draws, an odd number of SVM units were selected. We refer to this classifier methodology as Voting SVM. A similar approach was presented in [70]; however, their algorithm was applied to Common Spatial Pattern features and utilized Bagging to generate random sub-datasets for each SVM unit. Additionally, they omitted the use of any artifact rejection algorithm.

3.2.2.5 Epoch based Cross-validation

N-fold cross-validation was employed to evaluate the validity of feature extraction algorithms in conjunction with SVM classifiers.

Initially, data was partitioned into N distinct subsets. In each iteration, N-1 subsets were designated as the training set and one subset as the testing set. New instances of

classifiers were created, trained using the training set, and their classification performance was evaluated on the testing set. This process was repeated N times. The results of each iteration were recorded and the final accuracy was computed as the arithmetic mean of individual classification outcomes. We set N to 5 in all experiments.

Partitioning the data at the window level, in instances where windows overlap, rather than at the epoch level, may result in invalid accuracy and evoke the issue of overfitting. This is due to the fact that windows derived from the same epoch may be allocated to both the training and testing sets. This can constitute a significant error when dealing with highly overlapping windows, as it implies that nearly identical features are present in both sets. Consequently, we opted to partition the data at the epoch level rather than at the window level. This ensures that windows derived from a single epoch are used exclusively in either the training or testing set.

3.2.3 Subjects and Experimental Setup

For the real-time working BCI System, we required a subject with tetraplegia to serve as a pilot. To this end, we collaborated with MEREK, the Rehabilitation Centre for Physically Disabled People in Hungary.

3.2.3.1 Subjects

Two subjects applied (B. and C., both male) having C5 or higher spinal cord lesions. The injury of each pilot was confirmed and classified by a neurologist concerning the International Standards for Neurological Classification of Spinal Cord Injury. This pre-competition Medical Check was mandated by the organizers for all Cybathlon participants.

Pilot B was 44 years old and had an incomplete C5 Neurological level of injury (NLI). His Asia Impairment Scale (AIS) was B. The additional comments of the neurologist were: “Dysesthesia in palms. No muscle function in the non-key muscles either (on neither scale).”

Pilot C was 38 years old and had a complete C4 NLI, with AIS A, by the time of the experiments. The additional comments of the neurologist were: “Paresthesia in palms and foot. No muscle function in the non-key muscles either (on neither scale).”

Both offline and online experiments were conducted with the pilots to record our dataset, test the BCI system on them, and enable them to control the online game.

3.2.3.2 Ethical Permit

This study was carried out following the Declaration of Helsinki and national guidelines, with written informed consent obtained from all subjects. The study received approval from the United Ethical Review Committee for Research in Psychology (EPKEB reference number: 2018-54).

Prior to each experiment, subjects were informed about the experimental procedures and provided written consent.

3.2.3.3 Data Acquisition

Electroencephalography (EEG) data were recorded using a 64-channel ActiChamp amplifier system (Brain Products GmbH, Gilching, Germany) and an actiCAP EEG cap in accordance with the international 10-20 system (presented in Figure 3.2). The POz electrode was used as the reference, and data were acquired from 63 electrodes. During experimental preparation, the impedance of the EEG electrodes was measured and maintained below $30k\Omega$ Impedance values were recorded and saved along with the EEG data. The signals were captured with 500 Hz sampling frequency.

Subjects were seated approximately 110-130 cm from an LG Flatron L204WT-SF 20" wide LCD monitor. Experiments were conducted in rooms equipped with Faraday cage shielding as well as in common rooms without electrical shielding. The use of unshielded rooms was intended to simulate the environment that would be present during the Cybathlon 2020 competition.

Raw EEG signals were recorded using the BrainVision Recorder program (version: 1.22.0001) without additional software or hardware filters.

3.2.4 Two Choice Paradigm

This section presents the offline paradigm used for EEG recording with our pilots. The so-called Two Choice Paradigm was designed to simplify the execution of the Physionet task as our pilots reported difficulty in performing four-limb imagination during some experimental trials.

Prior to each experiment, pilots were instructed to avoid blinking, swallowing, clenching, or making any movements or facial expressions unrelated to the task during task periods. They were asked to repeatedly perform only the required MI tasks while the fixation cross was displayed on the screen. During rest periods, the paradigm control program presented the next task on the screen in written form. During these periods,

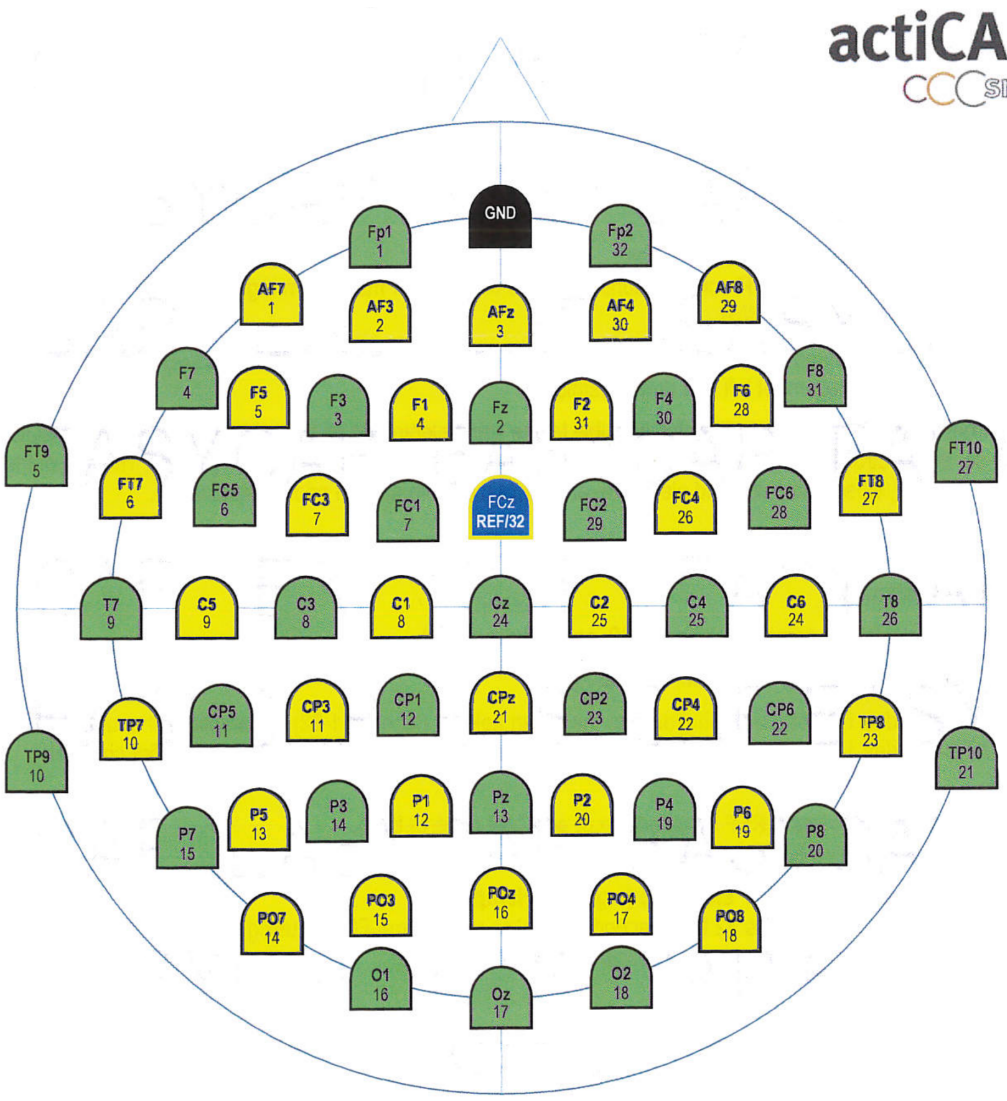

Figure 3.2. **Electrode placement** – During the experiments the POz electrode was used as the reference electrode instead of the original FCz. (Brain Products GmbH, Gilching, Germany)

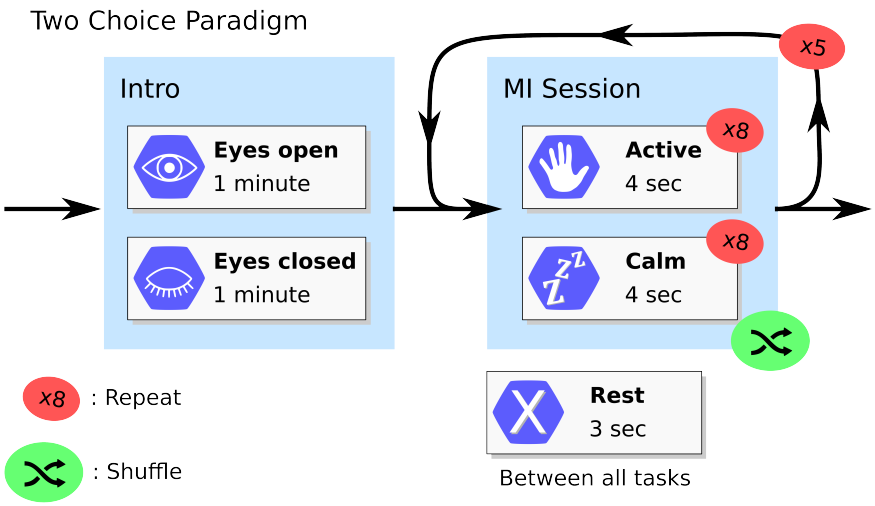

Figure 3.3. **Two Choice Paradigm** – It started with a one-minute open-eye and a one-minute closed-eye task, which served as a baseline and aimed to get the pilots' full attention, preparing them for the MI sessions. Under one MI session, 8 active and 8 calm mental tasks were required from the pilots. The order of the tasks was randomized. The MI session was repeated 5 times under one experiment.

pilots were permitted to blink, swallow, and make any necessary movements to prepare for the next task. Pilots were instructed to perform motor tasks for 4 seconds and rest tasks for 3 seconds.

The Two Choice Paradigm, illustrated in Figure 3.3, began with a one-minute period during which subjects were required to open their eyes and focus on the cross displayed on the screen. This was followed by a one-minute period during which subjects were instructed to close their eyes. In both cases, subjects were required to sit as calmly as possible, both physically and mentally, without engaging in any thoughts. This introductory session served as a baseline for the experiments and aimed to capture the pilots' full attention in preparation for the MI sessions.

Following the introductory session, the experiment consisted of 5 MI sessions. Here an active MI task and the calm task were required. Both tasks were presented 8 times per session in a randomized order. After each completed session, subjects were allowed to take a self-defined break without leaving the experimental setup.

For the active MI tasks, pilots were permitted to select and combine any hand and foot motor movements. However, these movements had to be decided upon and fixed prior to the start of the experiment. Pilot B selected Left Hand movements for the active task, while pilot C selected Both Feet movements. The calm task required subjects to sit

with their eyes open and refrain from making any movements or engaging in any thoughts or other potential sources of artifacts.

3.2.5 Offline Analyses

This section presents the methodology employed to compare features corresponding to EEG bands and to evaluate our BCI pipeline against the state-of-the-art EEGNet. These comparative analyses were conducted to determine the optimal configuration of the BCI system for real-time game control.

3.2.5.1 Investigating the Effects of EEG Bands on Classification Accuracy

To determine the optimal EEG bands for BCI control, an experiment was conducted in which several distinct signal processing and classification steps were performed. Each classifier received one of the investigated EEG bands: alpha, beta, gamma, theta, range30, or range40.

Experiments were conducted on both the Physionet dataset and our Two Choice Paradigm dataset. For the Physionet dataset, a 4-class classification was performed using the active MI tasks: Left Hand, Right Hand, Both Hands, and Both Feet. For the Two Choice Paradigm dataset, a 2-class classification was performed in which active MI imagination was classified against the calm phase.

Classification results for different EEG bands were collected and compared statistically. Repeated-measures ANOVA (rm-ANOVA) was performed for normally distributed data, followed by two-sided t-tests as post hoc tests. For non-normally distributed data, the Friedman test was used in place of rm-ANOVA and two-sided Wilcoxon signed-rank tests were used as post hoc tests. P-values were corrected using Bonferroni correction and the significance level was set at 0.05.

3.2.5.2 Comparison with EEGNet

EEGNet [31] was used as a benchmark to evaluate the accuracy and precision of our feature extraction and classification algorithms. The network was trained using 1-second-long EEG windows generated following FASTER artifact detection. The number of training epochs was set to 500, and an early stopping strategy was employed to prevent overfitting, with the patience parameter set to 20. Additionally, a custom strategy was used to save and restore the best network weights during testing: network weights

were saved if the validation accuracy was greater than or equal to the previous value and the corresponding validation loss was lower.

Comparisons between our method and the state-of-the-art EEGNet were conducted using both the Two Choice Paradigm and Physionet datasets. The normality of the accuracy results was assessed, and either a t-test or Wilcoxon test was used to determine significant differences between the methods based on the results of the normality test.

3.2.6 Online Paradigm and Experiments

Following the offline comparison of signal processing and classification algorithms, the most suitable configuration was selected for use in the real-time BCI system. An online paradigm was developed to record data for tuning the BCI system's classifier and to enable control of the game.

3.2.6.1 Online Paradigm

The online paradigm was designed to meet the requirements of the BCI race in the Cybathlon 2020 competition for subjects with tetraplegia (`https://cybathlon.ethz.ch/en/event/disciplines/bci`). The paradigm began with an offline training period used to calibrate the online game-playing phase. During this training period, the Two Choice Paradigm was conducted and the recorded data were used to train the BCI system's classifier. After the calibration, the BCI system was able to control the BrainDriver program provided by the organizers of the Cybathlon 2020 competition. This program managed the virtual environment and race conditions for the BCI discipline. A computer monitor displayed the game for the pilot, providing immediate visual feedback on the results of their mental commands.

The BrainDriver program required four input commands from the user (three active commands plus the absence of any commands), but the Two Choice Paradigm was designed to elicit only two. To bridge this gap, a unique mechanism called the Toggle Switch was introduced, inspired by the Brain Tweaker team [36]. When an active MI task was performed by the user, game control commands were cycled through in sequence at a predefined frequency. When the desired control command was reached, the user had to initiate a calm mental task to maintain that command and send no further commands to the game. This mechanism is illustrated in Figure 3.4.

Utilizing the Online Paradigm, a total of 16 experiments were executed with the participation of our two pilots.

3.2.6.2 BrainDriver Game

The BrainDriver software is a car racing-style video game developed for the BCI Race of the Cybathlon 2020 in collaboration with ETH Zurich and Insert Coin, Switzerland (`http://www.insert-coin.ch/`). Up to four players can compete simultaneously in the game. Each player controls an avatar that moves forward by default and must reach the finish line. The objective is to guide the avatar through the racetrack by providing properly timed mental commands in designated zones. If an incorrect command is given or no input is provided when required, the pilot's avatar slows down. Conversely, providing the correct control command restores the avatar's default speed.

The game features four types of track elements: Left Turn, Right Turn, Light On, and Straight Zone. In the Light On zone, player must turn on their vehicle's front light when the surrounding lights go off. In the Straight Zone, any command results in a slowdown of the avatar. The length of the game track was fixed at a virtual 500 meters by the Cybathlon organizers and includes four instances of each type of track element.

The BrainDriver game can be controlled using the UDP network communication protocol. Each player can send their control command as an unsigned byte code to the server's IP and port address.

A track generator program was developed for the game to randomize the order of different track elements such that a straight track element always followed a turn. This program was used prior to each experiment in the Online Paradigm to generate a new game track and prevent pilots from memorizing the path.

3.2.6.3 Real-time BCI System

Our real-time BCI system required pre-recorded training data obtained immediately prior to pilots playing the BrainDriver game. To acquire this data, the Online Paradigm was used to create the necessary dataset.

An RBF kernelled Voting SVM was used as the classifier for the BCI system. The classifier was trained offline using the range40 method with L2 normalization applied to 1-second-long windows with 0.1-second shifts.

Real-time EEG data were acquired from the amplifier using the Lab Streaming Layer (LSL) protocol [71]. Based on feedback from our pilots, one signal processing and decision-making step was performed every 1.6 seconds, corresponding to the periodic time for sending a game control command. During each decision-making step, the most recent 1-second of EEG data were treated as an EEG window and subjected to the same signal

processing and classification steps as the pre-recorded dataset: the range40 method was calculated with L2 normalization and input to the trained RBF kernelled Voting SVM for classification. The classification result was directly associated with a game control command (Figure 3.4) which was immediately sent to the game server's IP address and port number via UDP protocol. The implemented signal processing and classification methods were sufficiently fast for use in a real-time environment.

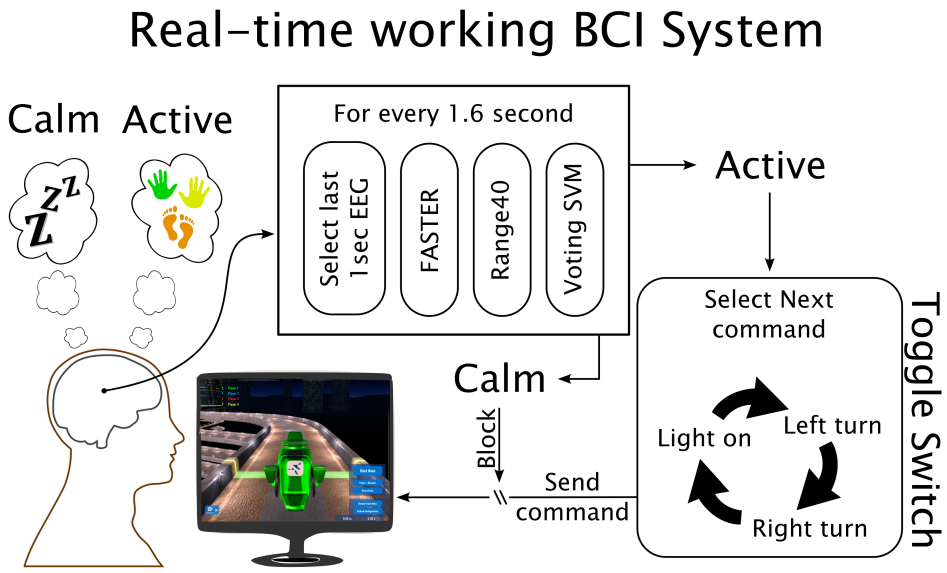

Figure 3.4. Components of our real-time BCI System and the Toggle Switch control mechanism.

Experiments with the real-time BCI system were conducted in a common room at the pilots' institution without electrical shielding to simulate a Cybathlon-like environment.

3.3. Results

In this chapter, we present our findings regarding the investigation of EEG bands on both the Physionet and our own Two Choice Paradigm datasets, recorded with the assistance of our pilots. We also report the results of comparing our Voting SVM classifier using the range40 feature with the state-of-the-art EEGNet. Additionally, we present results obtained using the real-time BCI application, in which we measured the time required for pilots to reach the finish line in the BrainDriver game.

3.3.1 Investigating the Effect of EEG Bands on Classification Accuracy

For the Physionet dataset, a 4-class classification was performed, while for the Two Choice Paradigm dataset, a 2-class classification was conducted. The accuracy of each classification was measured for each experiment using 5-fold cross-validation. The final accuracy for each dataset was determined as the average of all 5-fold cross-validated experimental accuracies for all subjects (Avg. Acc). These results are presented in Figure 3.5. Statistical tests were used to determine significant differences between EEG bands. Normality tests were first performed on the 5-fold cross-validated accuracies to determine the appropriate statistical tests to use.

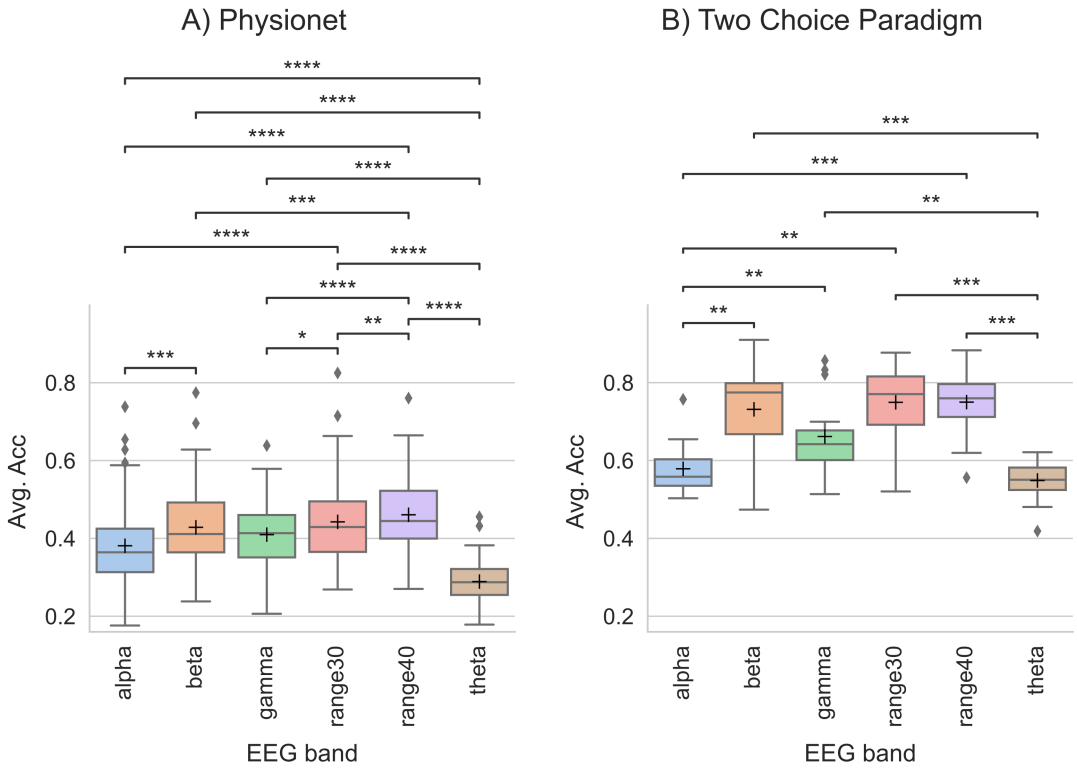

Figure 3.5. **EEG band effect investigation** – On both Physionet and the Two Choice Paradigm database, the impact of different frequency range based features were investigated and compared with each other statistically. The significant differences between the canonical EEG bands and the range30 and range40 methods are marked with stars. The p-value annotation legend is the following: *: $10^{-2} < p \leq 5 \times 10^{-2}$; **: $10^{-3} < p \leq 10^{-2}$; ***: $10^{-4} < p \leq 10^{-3}$; ****: $p \leq 10^{-4}$. The mean of the data is presented with the '+' symbol. The horizontal line in the box represents the median of the data. The box shows the quartiles of the dataset while the whiskers extend to show the rest of the distribution, except for individual points that are determined to be outliers.

Table 3.1 presents the results of normality tests, the type of main effect statistical tests used, and their corresponding p-values. The 5-fold cross-validated results were not normally distributed; therefore, Friedman tests were used on both the Physionet and Two Choice Paradigm datasets. The main effect was significant for both datasets, so Wilcoxon tests were used to determine which EEG band could produce significantly higher classification accuracies.

Table 3.1. Statistical test results of main effect on EEG band investigation

Database	**Normal distribution**	**Stat. test**	***p*-value**
Physionet	False	Friedman	$\mathbf{1.612 \times 10^{-45}}$
Two Choice Par.	False	Friedman	$\mathbf{1.533 \times 10^{-9}}$

As shown in Figure 3.5A for the Physionet dataset, the beta band achieved the highest accuracy among canonical EEG bands at 0.4285. It significantly outperformed all other canonical EEG bands except for gamma, which achieved an accuracy of 0.4097. However, when including range methods, range40 achieved significantly higher accuracy at 0.4607.

For the Two Choice Paradigm dataset, shown in Figure 3.5B, we obtained similar but less significant results compared to those for the Physionet dataset. The accuracies for beta, range30, and range40 were 0.7314, 0.7494, and 0.75 respectively. There were no significant differences between these EEG bands; however, this dataset contained only 16 experiments compared to 105 for the Physionet dataset after exclusion.

3.3.2 Comparision with EEGNet

We compared our Voting SVM classifier using the range40 method with the state-of-the-art EEGNet. For the Two Choice Paradigm dataset, the Voting SVM and EEGNet achieved accuracy levels of 0.7151 and 0.6857 respectively, while for the Physionet dataset, they achieved accuracy levels of 0.4866 and 0.4126 respectively. The distribution of results for EEGNet on the Physionet dataset was non-normal, so a Wilcoxon significance test was used with a preset significance level of 0.05. On the Physionet dataset, our Voting SVM with the range40 feature significantly outperformed EEGNet (p-value $< 10^{-4}$). However, there was no significant difference between the two methods on our Two Choice Paradigm dataset. The results of these comparisons are presented in Figure 3.6.

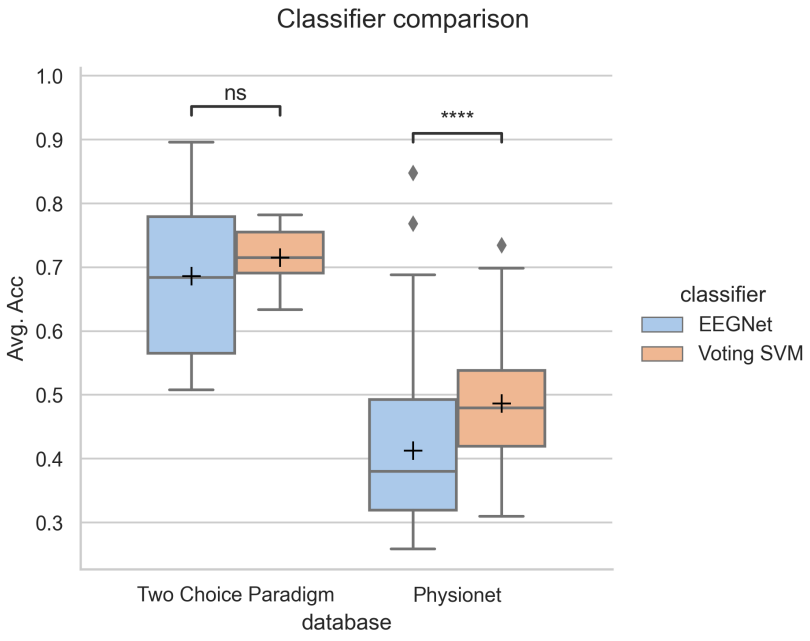

Figure 3.6. 5-fold cross-validated accuracy level comparison of range40 + Voting SVM with EEGNet. The p-value annotation legend is the following: non-significant (ns): $5 \times 10^{-2} < p$; ****: $p \leq 10^{-4}$. The mean of the data is presented with the '+' symbol. The horizontal line in the box represents the median of the data. The box shows the quartiles of the dataset while the whiskers extend to show the rest of the distribution, except for individual points that are determined to be outliers.

3.3.3 Real-time working BCI Experiment

Using the online paradigm, we conducted a total of 59 gameplay trials over 9 experimental days with the assistance of pilots B and C (pilot B - 24, pilot C - 35). The experiments were conducted in a common room at the pilots' institution without electrical shielding.

Each pilot played the BrainDriver game four times per experimental day. For each gameplay session, we measured the time required for the pilot to reach the finish line, as shown in Figure 3.7. The time limit of 240 seconds set by the organizers of the Cybathlon 2020 is indicated in red. A total of 27 gameplay sessions were completed within this time limit. We also present the learning curves for each pilot in Figure 3.7. Pilot B showed significant improvement (p-value $0.01 < 0.05$), although it should be noted that he was absent for three experiments. Pilot C showed an insignificant increasing learning curve (p-value $0.092 > 0.05$).

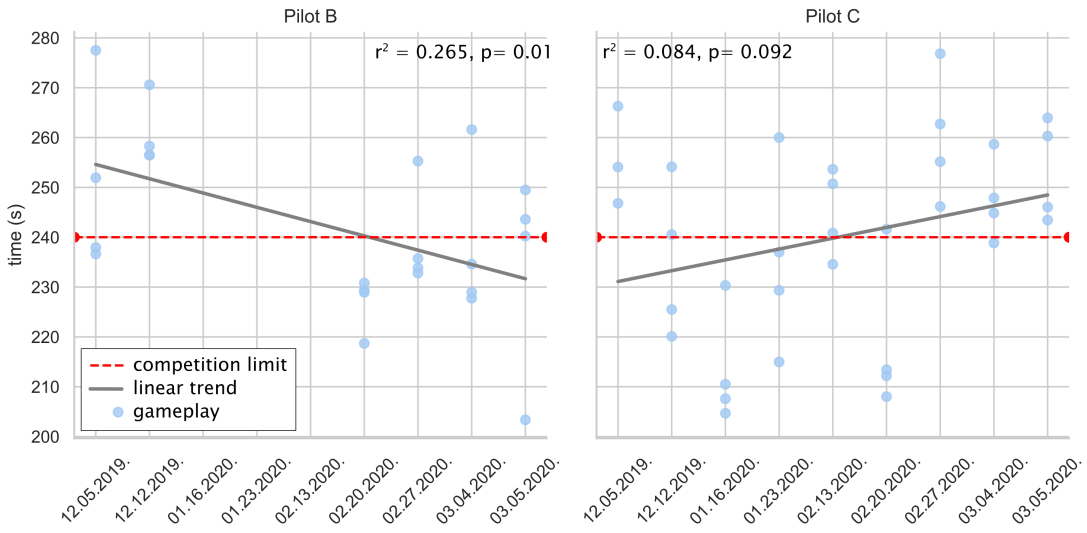

Figure 3.7. Gameplay performance of pilots per experimental day. 240 seconds were marked with a red line, which is the time limit defined by the organizers. The gray lines present the learning curves.

3.4. Discussion

In this study, we have presented the development of our BCI system for the Cybathlon 2020 competition. We chose to test our algorithms using the Physionet [54], [56] dataset rather than BCI competition datasets because it contains experimental data from 109 subjects, while others have fewer than 10. This allowed us to obtain reliable information about the performance of our algorithms and conduct significance comparisons.

In addition to the Physionet dataset, we created our own dataset for the real-time BCI system with the assistance of subjects with tetraplegia (referred to as pilots) who had spinal cord lesions at or above the C5 level. We designed a Two Choice Paradigm instead of a standard four-choice paradigm, as used in the Physionet dataset, because our pilots reported difficulty in performing four-limb imagination.

With regard to the BCI system, we implemented the FASTER algorithm [59] to meet the high requirements for artifact removal set by the Cybathlon organizers.

Our BCI system operates in the frequency domain. The absolute value of the FFT spectrum was calculated for 1-second-long EEG windows as a feature. From this FFTabs data, we either calculated the average between two frequencies or multiple averages from 2 Hz wide, non-overlapping frequency bins (referred to as the Feature Range method). In the case of the Feature Range method, multiple SVMs were trained, each receiving only one frequency bin. The final decision was determined by taking the maximum vote of all SVM units. We refer to this ensemble classifier as Voting SVM. To the best of our knowledge, Voting SVM combined with the range40 method based on FFTabs has not been previously investigated and compared statistically on MI datasets or used to control a computer game as part of a BCI application. A similar approach was reported in [70], but they used their algorithm on CSP features and employed Bagging to generate random sub-datasets for each SVM unit. Their MI tasks were left little finger and tongue movements, and they did not use any artifact rejection algorithm prior to signal processing. Their proposed algorithm was not compared with any other published signal processing or classification methods.

We conducted multiple comparison analyses on both the Physionet and our own datasets to determine the most suitable configuration for our BCI system. First, we compared different EEG bands and range30 and range40 methods statistically. On the Physionet dataset, among canonical EEG bands (alpha, beta, gamma, theta), beta achieved the highest accuracy level and significantly outperformed all other bands except

for gamma. However, when including range methods in the comparison, range40 significantly outperformed all other methods. As a result, we selected range40 with Voting SVM classifier for comparison with state-of-the-art EEGNet [31] algorithm to provide a broader perspective on our findings within the BCI community. According to Wilcoxon statistical tests, our method significantly outperformed EEGNet on the Physionet dataset. Repeating these tests on our Two Choice Paradigm dataset yielded less significant results.

The performance of EEGNet was initially reported on the BCI Competition IV 2a dataset [52], where it achieved an accuracy of 0.6547 for 4-class classification on 9 subjects. On the Physionet dataset, we obtained an accuracy of 0.4126 for 4-class classification on 105 subjects. These two analyses may not be directly comparable due to the larger number of subjects in the Physionet dataset and our use of the FASTER algorithm to filter artifacts from the source signals. To obtain statistically significant results about differences between classifiers, we recommend using datasets with large number of subjects. Our Two Choice Paradigm dataset comprises data from 16 experimental sessions, collected with the participation of 2 subjects with tetraplegia. This may account for the lack of statistically significant difference between EEGNet and Voting SVM on this dataset.

After conducting these comparisons, we developed a real-time BCI system that includes a unique control protocol called the Toggle Switch. This algorithm allowed our pilots to control the BrainDriver computer game using only two mental commands instead of four. Our approach was inspired by Perdikis et al. [36], who developed an algorithm that classified two MI signals using a thresholding technique. When a third active game control command was required, their pilot initiated two different active MI tasks within a given time window. In contrast, our method cycles through active control commands one after another when our pilots initiate an active MI task, allowing for easy extension with additional commands.

Using the Online Paradigm and our BCI system, we conducted real-time BCI experiments with our pilots using the BrainDriver game developed for the BCI discipline of the Cybathlon 2020 competition. During these gameplay sessions, pilots received immediate feedback from the computer about the correctness of their mental commands. Our pilots completed the game with varying runtimes between 200 and 280 seconds, as shown in Figure 3.7. Pilot B showed a significant learning curve, while Pilot C faced difficulties. Nevertheless, the latter was statistically insignificant. Due to pandemic-related restrictions, we were only able to conduct 9 experimental days resulting in a total of 59 gameplay

trials for both pilots. To further investigate the learning effect, additional experiments with the Online Paradigm would be required, which is considered as a limitation of our research.

To provide context for our work, we present results from other Cybathlon teams that participated in either the Cybathlon BCI Series 2019 or the Cybathlon 2020 event. The Nitro1 team [64] focused on minimizing within- and between-session variability and shifts using the Riemann framework. They projected generated features onto a common reference before performing classification using a Minimum Distance to Mean classifier. Their 4-class BCI system included two MI classes (Left Hand and Right Hand), mental subtraction, and an idle state. A blinking detector and thresholding technique applied to absolute EEG signals were used to reject features containing artifacts. While their approach showed increasing classification accuracies, this was not reflected in their game performance as measured by time required to reach the finish line. Most of their runs exceeded 250 seconds, whereas most of ours were below this threshold.

Team SEC FHT [65] implemented an artifact removal algorithm that detected EOG artifacts using Pearson's correlation and interpolated affected channels. FBCSP was calculated on the purified EEG data and a Gaussian-kernelled Support Vector Machine (SVM) was used for classification. Four MI tasks (Left Hand, Right Hand, Both Feet, Rest) were used to elicit control signals. The team investigated the precision of their control system with respect to the training protocol, comparing offline arrow-based, offline game-based, and online gameplay training. They achieved their best performance using training data derived from online gameplay, where the pilot received immediate feedback about the correctness of their commands. However, even when using their best method (training the classifier on data from previous gameplays), their gameplay results showed similar fluctuations to ours, with finish times ranging from 210 to 310 seconds.

The most significant improvements in BCI performance were reported by teams MIRAGE91 [39] and WHI [37], both of which achieved regression p-values below 0.001 for their learning curves. The performance range of team MIRAGE91 (160-300 seconds) is comparable to our results. However, team WHI outperformed all other teams, with competition times starting at 280 seconds and decreasing to 160 seconds.

Additional Cybathlon BCI topics can be found in [66], [72]–[74].

3.5. Conclusion

In this part of the dissertation, we presented a novel ensemble SVM classifier, termed Voting SVM, incorporating the range40 feature. To our knowledge, this configuration has not been previously utilized in MI-based BCI applications. Our signal processing and classification algorithm were rigorously evaluated using the Physionet dataset and demonstrated superior performance compared to the state-of-the-art EEGNet classifier.

We introduced the Two Choice Paradigm with a unique Toggle Switch control mechanism in our real-time BCI system for controlling the BrainDriver computer game. A total of 59 gameplay trials were conducted with two pilots, both diagnosed with C5 or higher spinal cord lesions. Our results, in terms of online gameplay, were comparable to those of other teams participating in Cybathlon 2020.

Future work will involve continued experimentation and data collection to expand our existing dataset. This will provide an opportunity to further develop our BCI system by incorporating additional features and normalization techniques and exploring the use of neural networks alongside EEGNet. Additionally, we plan to focus on subject learning, as it has been shown to significantly impact the robustness of BCI systems [36].

Despite challenges, our efforts have yielded promising results. As such, we intend to participate in the next Cybathlon event in 2024.

10.15774/PPKE.ITK.2024.001

Chapter 4

Deep Comparisons of Neural Networks from the EEGNet Family

4.1. Introduction

Artificial Neural Networks made a seminal contribution to the field of BCI when Schirrmeister et al. [75] introduced Deep ConvNet and Shallow ConvNet in 2017 for EEG signal classification. Subsequently, neural networks have emerged as one of the most prominent topics in BCI literature.

When a novel system is developed for MI signal classification, it is frequently evaluated and contrasted with previously published systems utilizing one of the BCI Competition databases: [49]–[52]. However, these datasets encompass records from a limited number of subjects, typically less than or equal to 10. Other open-access databases contain EEG records from more than 50 subjects but are predominantly avoided by researchers. One such database is the MI EEG dataset on PhysioNet [54] recorded using BCI2000 software [56], which comprises EEG records from 109 subjects. Another database was recorded using the OpenBMI toolbox [76] and contains data from 52 subjects, each of whom participated in two experimental days. Additionally, we have recorded our own dataset, which includes 25 experiments from 9 subjects [Au6]. Concerning the referenced literature of chapter 4, 39 instances employ one of the BCI Competition datasets, whereas a mere 6 instance utilize the MI EEG database available on PhysioNet. We presume that databases with more than 20 experimental days are sufficient for BCI system comparison.

Prior to the advent of neural networks, researchers endeavored to investigate and develop hand-crafted feature extraction methods in conjunction with simple classification algorithms. Blankertz et al. [77] successfully employed the CSP algorithm with an

LDA classifier to control a cursor in one dimension. Barachant et al. [78] introduced Riemannian geometry for BCI with an LDA classifier, effectively classifying EEG covariance matrices. Lotte and Guan [21] proposed a unifying theoretical framework for regularizing the CSP and compared it with 10 other regularized versions of the CSP algorithm. Another feature extraction algorithm, based on the CSP, is the FBCSP with a naïve Bayesian Parzen window classifier [22], which was compared with the ConvNets [31], [75] on the BCI Competition IV 2a database. The winner of the BCI discipline of the Cybathlon competitions used the utilized power spectral density of the EEG signals as a feature [36], [37] with a Gaussian classifier.

The introduction of Deep and Shallow ConvNets heralded a new trend in BCI development, shifting the focus from hand-crafted features to the creation of neural networks that not only classify signals but also incorporate the feature extraction step. Lawhern et al. [31] introduced EEGNet, drawing inspiration from previous neural networks designed for EEG signal processing, including MI-based BCIs [26], [75], [79], [80]. It was demonstrated that EEGNet performs feature extraction similar to FBCSP. This neural network inspired numerous researchers, resulting in the development of many improved versions of EEGNet, culminating in the creation of an entire family (Table 4.1) of neural networks.

Several publications outside of the EEGNet family have underscored the importance of research on neural-network-based BCIs. Dokur and Olmez [91] presented a minimum distance network capable of learning at a faster rate than other deep neural networks. Fadel et al. [Au2], [Au3] explored the classification of image-like EEG data, while Han et al. [27] focused on the development of parallel network architecture. Jia et al. [92] introduced a joint spatial–temporal architecture, which was further developed in [93] and successfully applied to cross-subject classification. Roy demonstrated [94] that classification accuracy can be further enhanced through the utilization of transfer learning.

Along with the development of neural networks, scientists started investigating the impact of transfer learning [95]. This methodology aims to transfer knowledge between two domains and increase classification accuracy. Khademi et al. [96] employed a CNN-LSTM hybrid model, which was pretrained on the ILSVRC subset of the ImageNet dataset to classify MI EEG signals. Their objective was to transfer knowledge from image classification and apply it to spatial EEG images generated using the CWT method with a complex Morlet mother wavelet. Another approach is to utilize the entire EEG dataset and combine cross-subject and within-subject training, as demonstrated in [94], [97], [98].

Table 4.1. EEGNet family and the used MI EEG databases

Neural Network	**Used MI EEG database**
Shallow ConvNet [75]	BCI Competition IV dataset 2a and 2b
Deep ConvNet [75]	BCI Competition IV dataset 2a and 2b
EEGNet [31]	BCI Competition IV dataset 2a
S-EEGNet [81]	BCI Competition IV dataset 2a
EEGNet Fusion [42]	PhysioNet
TCNet Fusion [82]	BCI Competition IV dataset 2a, High Gamma Dataset
Sinc-EEGNet [55]	BCI Competition IV dataset 2a
TSGL-EEGNet [83]	BCI Competition IV dataset 2a, BCI Competition III dataset IIIa
MI-EEGNet [40]	BCI Competition IV dataset 2a, High Gamma Dataset
Channel-Mixing-ConvNet [84]	BCI Competition IV dataset 2a, High Gamma Dataset
AMSI-EEGNet [63]	BCI Competition IV dataset 2a
ATCNet [85]	BCI Competition IV dataset 2a
FFCL [86]	BCI Competition IV dataset 2a
MTFB-CNN [87]	BCI Competition IV dataset 2a and 2b, High Gamma Dataset
TCACNet [88]	BCI Competition IV dataset 2a, High Gamma Dataset
FB-EEGNet [89]	No MI databases are utilized
CRGNet [90]	BCI Competition IV dataset 2a

In this case, knowledge is transferred from subjects whose data were not included in the neural network's test set. The network is pre-trained on data from all but one subject, as in a cross-subject training procedure. However, the data of the test subject is also partitioned into training and test sets, as in within-subject training, and the training portion is used to fine-tune the pre-trained neural network. We opted for the latter version of transfer learning because it is architecture-independent and intended to apply it following artifact filtering.

In this study, all the experiments were conducted on data purified of artifacts because eye and muscle movement activity can distort the EEG signals [59]. This is attributable to the fact that the amplitude of electromyographic signals can be orders of magnitude greater than EEG signals. Furthermore, it has been demonstrated that artifacts can be successfully utilized for BCI purposes [99]; however, in our view, a genuine BCI should not rely on artifacts but solely on pure EEG signals. In addition, concerning a prominent international BCI competition, the Cybathlon "bionic Olympics" [35], participating BCI teams are required to implement an online artifact removal algorithm.

To reduce computational time for experiments, we arbitrarily selected Shallow and Deep ConvNet [75] as predecessors of EEGNet, the EEGNet itself [31], the EEGNet Fusion [42], and the MI-EEGNet [40] from the EEGNet family.

4.2. Materials and Methods

This section presents the databases and neural networks, along with the experimental setups and concepts. The code utilized in this study is accessible at: `https://github.com/kolcs/bionic_apps`

4.2.1 Databases

We present the datasets employed for the EEGNet family comparisons. The databases were processed in an "independent days" configuration, meaning that if a subject participated in an experiment multiple times on different experimental days, the data were treated as if they had been recorded from distinct subjects. To our knowledge, EEG data can be significantly influenced by numerous factors, including recording setup, time of day, and the mental state of subjects, as also demonstrated in [100]. These could all lead to poorer performance if the data is merged concerning the subjects. It was also demonstrated in [101] that there is a great difference in cross-experimental day classification. With the independent days configuration, we aimed to overcome this problem and extend

the number of subjects to strengthen the results of the statistical analyses, similar to in [102].

4.2.1.1 Physionet

The Physionet dataset, which is sampled at a frequency of 160 Hz across 64 channels without the employment of hardware filters and comprises four Motor Imagery (MI) signals, is expounded in detail in Section 3.2.1.

4.2.1.2 Database on Giga Science

Lee et al. [76] published an EEG dataset that included three paradigms: MI, event-related potential, and steady-state visually evoked potential. The experimental paradigms were conducted using the OpenMBI toolbox, custom written in MATLAB. We selected the files corresponding to the MI EEG paradigm from these three paradigms, which contains a 2-class classification problem, involving the imagination of Left Hand and Right Hand movement. The EEG signals were recorded using a 62-channeled BrainAmp amplifier system with a sampling rate of 1000 Hz. Fifty-four subjects participated in the experiments; each subject was present on two distinct experimental days. Therefore, in accordance with our independent days configuration, this dataset contains data from 108 subjects. To reduce the size of the raw EEG files, we resampled the data to a sampling frequency of 500 Hz. For convenience, we will refer to this specific dataset as the Giga database.

4.2.1.3 BCI Competition IV 2a

Tangermann et al. [52] introduced the well-known and widely utilized BCI Competition IV database, which includes 5 sub-datasets with varying paradigms and challenges. This popular dataset is employed as a benchmark in the BCI literature to evaluate the developed methods and algorithms. In this study we utilize only the 2a sub-dataset, an MI dataset with Left Hand, Right Hand, Both Feet, and Tongue tasks. The EEG signals were recorded with a 250 Hz sampling frequency on 22 electrodes. The amplifier included a hardware bandpass filter between 0.5 and 100 Hz, and a notch filter at 50 Hz to remove the powerline noise.

This dataset was recorded with the assistance of 9 experimental subjects and each subject participated in two different experimental days. Therefore, concerning the independent days configuration, this dataset contains 18 subjects.

4.2.1.4 TTK

The TTK database [Au6], recorded at the Research Centre for Natural Sciences (TTK, as a Hungarian abbreviation), utilized a 64-channeled ActiChamp amplifier system (Brain Products GmbH, Gliching, Germany) to capture EEG signals at a sampling frequency of 500 Hz.

The EEG signals were recorded using a custom-built, MATLAB-based, paradigm leader code, General Offline Paradigm (GoPar), which was presented in the Supplementary Materials of [J1] and is accessible at `https://github.com/kolcs/GoPar`, and also presented in Figure 4.1.

This code, inspired by the paradigm of the Physionet database, was designed to conduct multiple different MI paradigms with four tasks: Left Hand, Right Hand, Left Foot, and Right Foot. The paradigm began with an initial task consisting of a one-minute eye-open session followed by a one-minute eye-closed session, intended to capture the subjects' full attention and prepare them for the core part of the experiment while serving as a baseline. Subsequently, two warmup sessions were conducted in which two of the four MI tasks were selected and practiced overtly and covertly to guide subjects on how to execute MI tasks. In total 25 experiments were conducted with 9 subjects. No hardware or software filters were applied during the EEG recording.

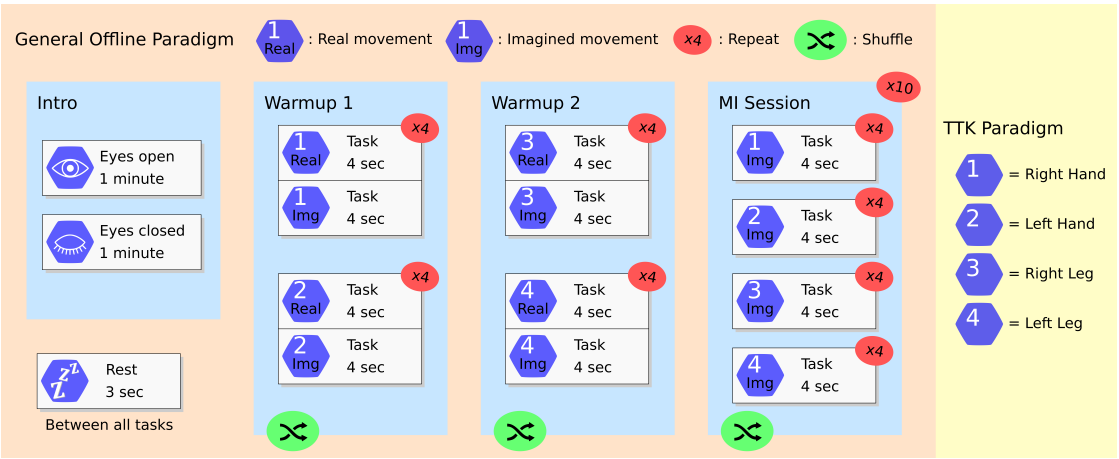

Figure 4.1. GoPar with TTK paradigm

4.2.2 Signal Processing

Initially, EEG signals were filtered with a 5th-order Butterworth bandpass filter in the range of 1 to 45 Hz. Subsequently, a customized FASTER algorithm [59], as described

in [J1] and section 3.2.2.1, was employed to eliminate EEG epochs and channels, which are contaminated by eye movements or muscle activity.

The resulting 4-s epochs were divided into 2-s windows with 0.1-s shifts to increase the sample size. The signals were then normalized using standard scaling, where the mean was set to zero and the standard deviation to one. These processed EEG windows were utilized for training and testing the classifiers of the BCI system.

For within-subject classification, 5-fold cross-validation was performed on a subject-wise basis, with the database split at the epoch level to ensure that windows originating from the same epoch were used exclusively in either the training or testing set. Approximately 10% of the training data was used as a validation set, with the split performed at the epoch level.

4.2.3 Neural Networks

This section describes the neural networks utilized in this study, as well as the methods and modifications employed in relation to the original networks.

4.2.3.1 Callbacks

During the training of the neural networks, a modified early stopping and model-saving strategy was implemented. The conventional early stopping approach [103] involves monitoring the validation loss and halting the learning process when it increases to prevent overfitting of the network. A patience parameter can also be specified to determine the number of training epochs that should elapse before the monitored value shows improvement. We extended this strategy by introducing an additional patience-like parameter termed "give up." This strategy is intended to address training scenarios in which the validation loss increases above the initial training loss but subsequently decreases as the neural network begins to learn. The give up parameter specifies the number of training epochs that should elapse before the validation loss returns to its initial value. If the initial loss is reached within the give up limit, the original patience value is activated; otherwise, training is terminated.

Our model-saving strategy was designed to reflect our modified early-stopping approach. Until the initial validation loss was reached, model weights with the highest validation accuracy were saved. After reaching the initial validation loss, model weights were only saved if improvements were observed in both validation loss and validation accuracy. Prior to testing, the best model weights were restored.

Our experiments were conducted with a maximum of 500 training epochs, a give up value of 100, and a patience value of 20.

4.2.3.2 ConvNets

The Deep and Shallow ConvNets [75] are built on traditional image processing convolution–max-pooling blocks. The Shallow ConvNet contains only one, as presented in Figure 4.2, while Deep ConvNet built up from four (Figure 4.3). The Deep and Shallow ConvNets were implemented using the source code provided in [31] which employs several modified parameters relative to those originally published in [75]. No further modifications were made to the architecture of the networks.

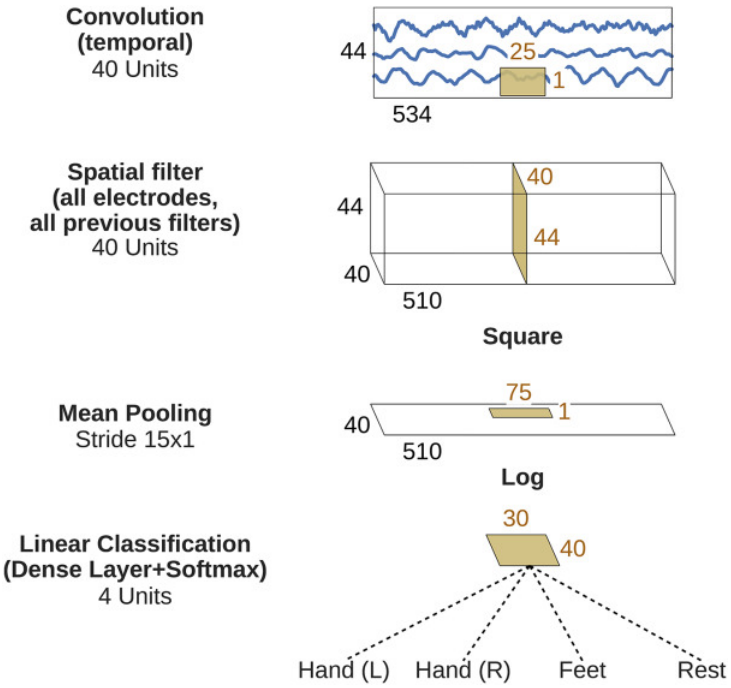

Figure 4.2. Shallow ConvNet architecture [75]

4.2.3.3 EEGNets

The architecture of EEGNet [31] (Figure 2.8) includes not just 2 dimentisonal temporal convolutional blocks, as the ancestor Deep- and Shallow ConvNet, but also depthwise- and separable convolutions as presented in the last paragraph of Section 2.5.3. EEGNet Fusion [42] (Figure 4.4) utilize 3 EEGNets with different kernel parameters to capture multiple representations of the original signal. On the other hand, the MI-EEGNet [40] (Figure 4.5) inserts a new part containing parallel separable convolution blocks right before the original separable convolutional block in the EEGNet.

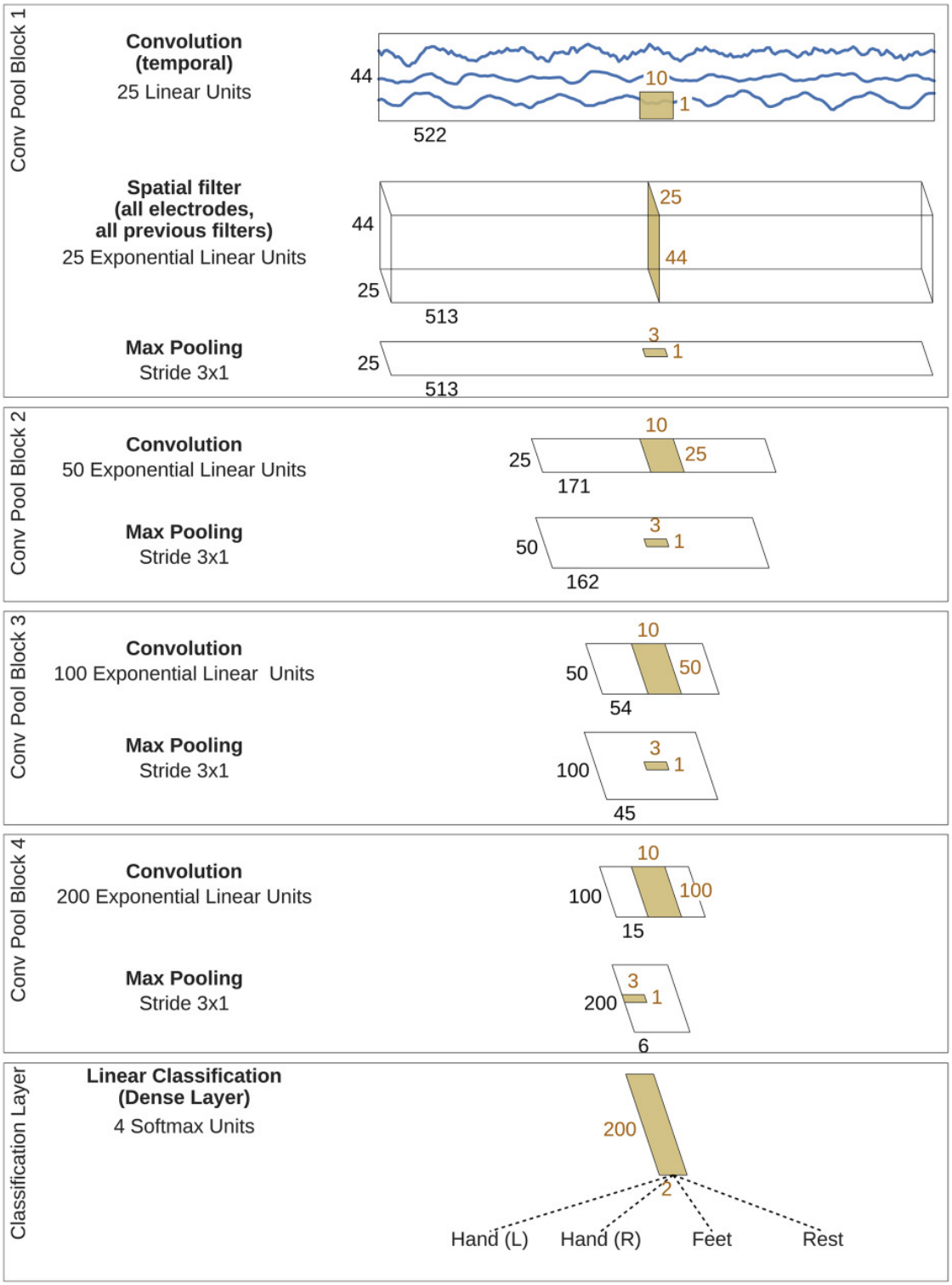

Figure 4.3. Deep ConvNet architecture [75]

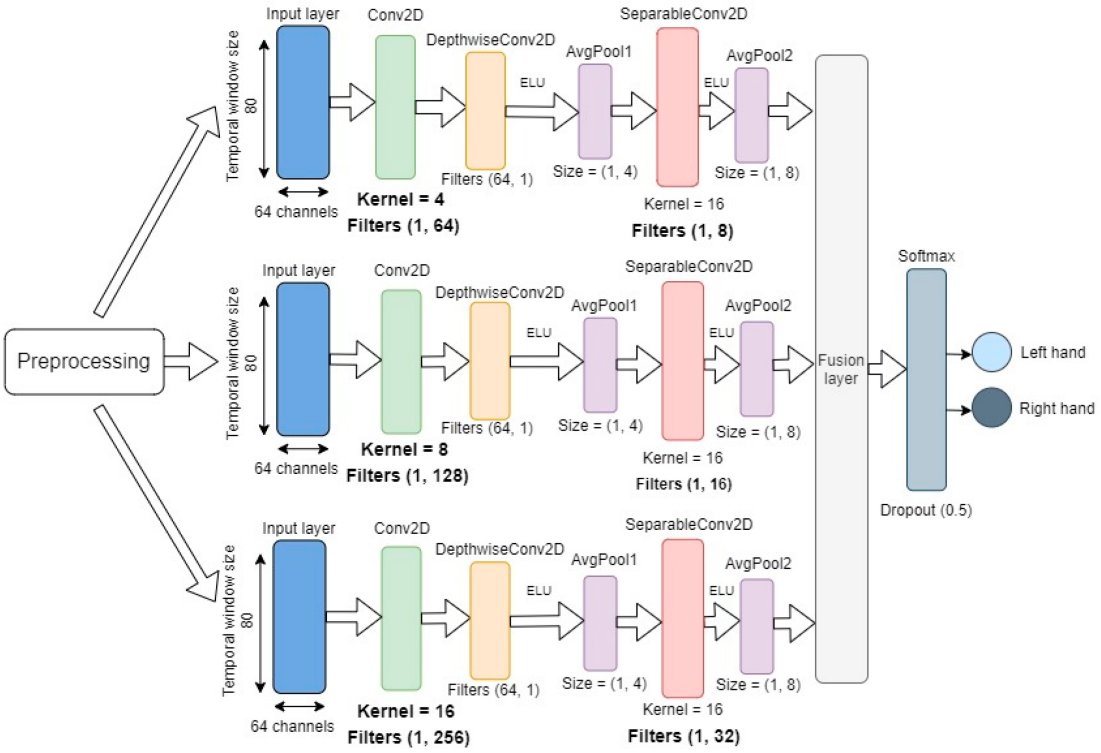

Figure 4.4. EEGNet Fusion architecture [42]

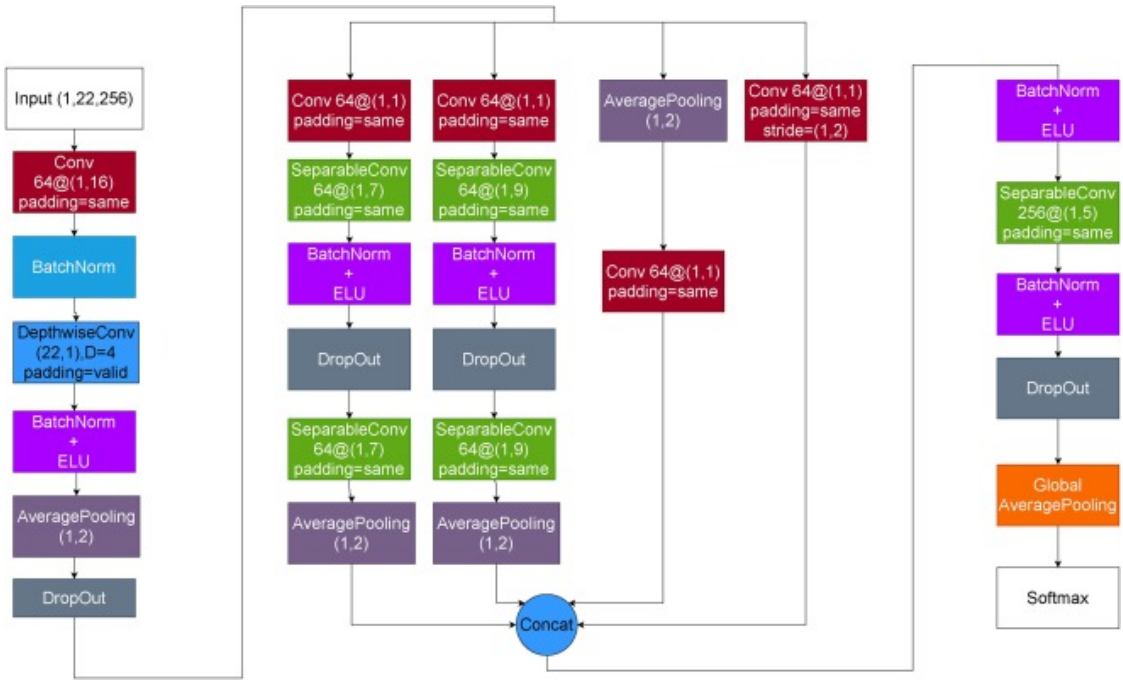

Figure 4.5. MI-EEGNet architecture [40]

The networks of the EEGNet family were slighthly modified in this study to enable automatic adaptation to databases with varying sampling frequencies, rather than requiring manual specification of input parameters. In the EEGNet publication [31], the authors explicitly stated that the filter size of the first convolutional block should be half of the sampling frequency. Accordingly, in our implementation, the kernel size was calculated based on the sampling frequency of the input signals, rather than being directly specified. This approach was also applied to EEGNet Fusion and MI-EEGNet.

4.2.4 Transfer Learning

In general, transfer leaning aims to utilize the knowledge of a source domain in a target domain as presented by Weiss et al. in [95]. This is practically useful, when few data is available in the source domain, therefore the training may not be sufficient, leading to overfitting.

In case of EEG signal classification the data of unused subjects, as in subject-wise learning, could be utilized to find optimal initial weights of the network, compared to a random initialized ones. Therefore, next to subject-wise learning, we also investigated the effects of transfer learning. Test subjects were selected as distinct groups of 10, with the remaining subjects designated as pre-train subjects and used to establish the initial optimal weights for the neural networks. A validation set was separated from the pre-train data for use with our modified early stopping and model-saving strategy. Upon convergence of the pretraining phase, either through reaching the maximum number of training epochs or through early stopping, the best network weights were stored. For each test subject, 5-fold within-subject cross-validation was performed as described in the third paragraph of Section 4.2.2. Prior to each cross-validation step, the saved model weights were loaded and the selected training set for the test subject was used as fine-tuning data for the neural networks. During fine-tuning, validation sets were again employed in conjunction with our early stopping and model-saving strategies.

4.2.5 EEGNet Family Comparison

Extensive computational experiments were conducted on each database (Physionet, Giga, TTK, and BCI Competition IV 2a) to compare the performance of the neural networks from the EEGNet family (Shallow ConvNet, Deep ConvNet, EEGNet, EEGNet Fusion, MI-EEGNet). In cases where a subject participated in multiple experiments on different days, the data was treated as if it had been collected from multiple subjects, referred to

as the independent days configuration. However, for the BCI Competition IV 2a dataset, we also conducted experiments in which data from a single subject was combined across recording dates to facilitate comparison with previous BCI studies. These experiments are denoted as "merged subject data."

Both within-subject and transfer learning phases were conducted for each neural network and database. Cross-validation results were collected and normality tests were performed to determine the appropriate statistical test (t-test or Wilcoxon) for normally or non-normally distributed accuracy levels, respectively. The resulting p-values were adjusted using Bonferroni correction, with a preset significance level of 0.05.

In addition to comparing accuracy levels, we introduced two additional metrics to rank the performance of the neural networks. These metrics were evaluated on databases configured for independent days. The first metric measures the improvement in accuracy achieved by the EEGNet family relative to chance level, which can be applied to databases with varying numbers of classes. This metric was calculated and averaged for both within-subject and transfer learning. The second metric assesses the effect of transfer learning by comparing the results of within-subject classification with those of transfer learning classification. The difference between the two methods was calculated for each database configured for independent days.

4.2.6 Statistical Investigation of Databases

To quantitatively evaluate our assumption that databases with more than 20 experimental days are sufficient for BCI system comparison, we investigated the number and quality of significant differences between databases. For each database configuration, two values were calculated: the sum of significance levels, as categorized in Table 4.2, and the count of significant differences. These values were then correlated with the number of subjects in each database.

Table 4.2. Levels of significance tests.

Level	***p*-Value Range**
1	$10^{-2} < p <= 5 \times 10^{-2}$
2	$10^{-3} < p <= 10^{-2}$
3	$10^{-4} < p <= 10^{-3}$
4	$p <= 10^{-4}$

4.3. Results

Upon obtaining five-fold cross-validated accuracy levels for all combinations of the four databases, five neural networks, and two learning methods (within-subject and transfer learning), normality tests indicated a non-normal distribution of the data. Consequently, the Wilcoxon statistical test with Bonferroni correction was employed for significance analysis. The results are presented in Figures 4.6 and 4.7. In general, transfer learning was found to significantly improve performance across all databases except for BCI Competition IV 2a.

For the Physionet database (Figure 4.6A), within-subject classification using MI-EEGNet yielded the highest accuracy (0.4646) relative to other methods, while transfer learning using Deep ConvNet achieved the highest performance (0.5377).

For the Giga database (Figure 4.6B), MI-EEGNet achieved the highest accuracies of 0.725 and 0.7724 for within-subject and transfer learning, respectively. This network significantly outperformed other networks, with the exception of Shallow ConvNet in transfer learning mode.

Analysis of results from the TTK dataset (Figure 4.6C) revealed that EEGNet achieved the highest accuracies of 0.4437 and 0.4724 for within-subject and transfer learning, respectively. These results were significantly higher than those obtained using other networks, with the exception of MI-EEGNet.

For the BCI Competition IV 2a dataset, when treated as independent days (Figure 4.6D), Shallow ConvNet achieved accuracies of 0.719 and 0.733 for within-subject and transfer learning, respectively. In transfer learning mode, this network significantly outperformed other networks; however, its performance was comparable to that of EEGNet and MI-EEGNet in within-subject classification mode. When data from a single subject was merged across experimental days, Shallow ConvNet again achieved the highest accuracies of 0.749 and 0.7533 for within-subject and transfer learning, respectively; however, differences between networks were not significant.

To establish a hierarchy among the neural networks, we analyzed the improvement in accuracy achieved by the EEGNet family relative to chance level. Table 4.3 presents the ranking of these networks based on their training modes. Across all databases configured for independent days, MI-EEGNet exhibited the greatest average improvement in within-subject classification, while Shallow ConvNet outperformed other networks in transfer learning mode.

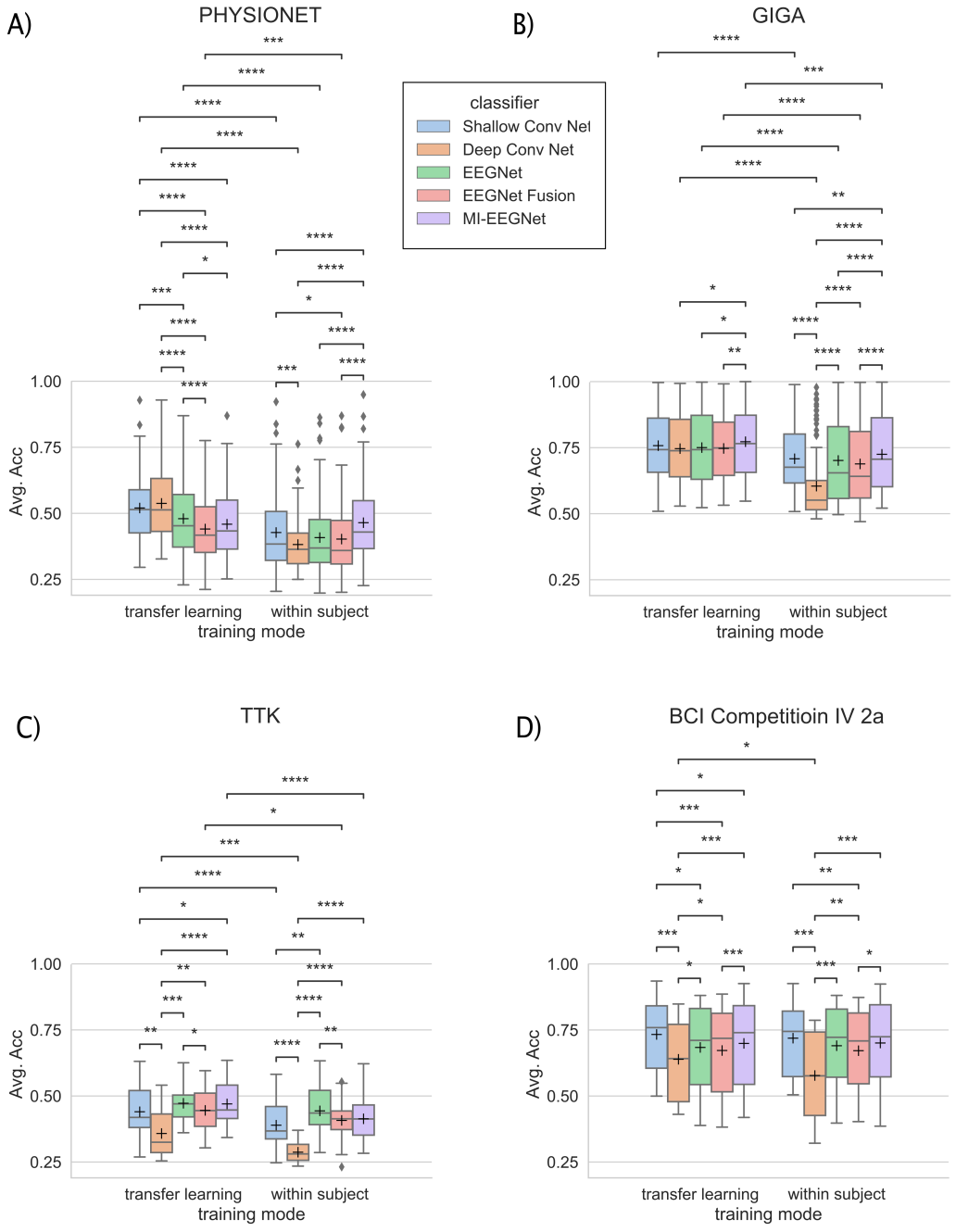

Figure 4.6. EEGNet family comparison on 4 databases handling the datasets in independent days configuration.

The p-value annotation legend is the following: *: $10^{-2} < p <= 5 \times 10^{-2}$; **: $10^{-3} < p <= 10^{-2}$; ***: $10^{-4} < p <= 10^{-3}$; ****: $p <= 10^{-4}$. The mean of the data is presented with the '+' symbol. The horizontal line in the box represents the median of the data. The box shows the quartiles of the dataset while the whiskers extend to show the rest of the distribution, except for individual points that are determined to be outliers.

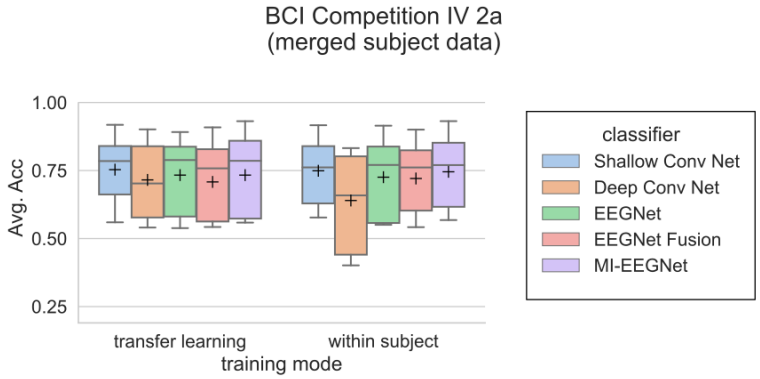

Figure 4.7. EEGNet family comparison on BCI Competition IV 2a. The statistical tests gave insignificant results. The mean of the data is presented with the '+' symbol. The horizontal line in the box represents the median of the data. The box shows the quartiles of the dataset while the whiskers extend to show the rest of the distribution, except for individual points that are determined to be outliers.

Table 4.3. Ranking the performance of neural networks on all the databases concerning the independent days configuration.

	Classifier	**Avg. Acc. Improvement from Chance Level**	**Rank**
Within subject	Shallow ConvNet	0.2071	2
	Deep ConvNet	0.1249	5
	EEGNet	0.1997	3
	EEGNet Fusion	0.1871	4
	MI-EEGNet	0.2306	1
Transfer learning	Shallow ConvNet	0.2721	1
	Deep ConvNet	0.2598	2
	EEGNet	0.2521	4
	EEGNet Fusion	0.2312	5
	MI-EEGNet	0.2537	3

We also considered the extent to which neural network performance was enhanced by transfer learning, as presented in Table 4.4. Deep ConvNet exhibited the greatest improvement, achieving results that were on average 0.1 higher than those obtained using within-subject classification mode. In contrast, Shallow ConvNet, which ranked first in transfer learning performance, improved by only 0.05 relative to within-subject classification.

Table 4.4. Classification improvements by transfer learning on databases with independent day configuration.

Rank	**Neural Networks**	**Physionet**	**Giga**	**TTK**	**BCI Comp IV 2a**	**Avg. Impr.**
1	Deep ConvNet	0.1557	0.1418	0.0708	0.0614	0.1075
2	Shallow ConvNet	0.0928	0.0497	0.0509	0.0141	0.0519
3	EEGNet	0.0716	0.0487	0.0288	−0.0065	0.0357
4	EEGNet Fusion	0.0381	0.0586	0.0379	0.0007	0.0338
5	MI-EEGNet	−0.0058	0.0475	0.0564	−0.0015	0.0241

Finally, databases were ranked based on the number of significant differences observed between them. Table 4.5 presents the sum of significance ranges (corresponding to the number of stars in figures) and count of significant differences alongside the number of subjects in each database. The sum of significance ranges was found to be strongly correlated with the number of subjects in each database ($r(3) = 0.7709$), although this correlation was not statistically significant (p-value $= 0.127014 > 0.05$).

Table 4.5. Significance investigation.

	Significance Level		
Database	**Sum**	**Count**	**Subjects**
Physionet	63	18	105
Giga	49	15	108
TTK	45	16	25
BCI Comp IV 2a	31	15	18
BCI Comp IV 2a-merged subject data	0	0	9

4.4. Discussion

Many articles presenting MI EEG signal classification using artificial neural networks from the EEGNet family report and compare their results on one of the BCI Competition databases, as presented in Table 4.1. The aim of this study was to demonstrate the necessity of using datasets with large numbers of subjects for statistically significant comparisons. To this end, we compared the performance of five neural networks from the EEGNet family on four databases containing data from various subjects. With respect to the datasets, we introduced an independent day configuration in which data from a subject who participated in multiple experimental days were treated as if they had been collected from multiple subjects. This configuration was intended to increase the number of experiments and enhance the significance of comparisons. All four databases, namely BCI Competition IV 2a database [52], Physionet [54], [56], Giga [76], and our TTK dataset [Au6], were used in this configuration. For the Physionet database, the authors reported that experiments were conducted with 109 volunteers, rendering the independent subject configuration irrelevant. For the BCI Competition IV 2a database, we also conducted an experiment in which data from a single subject was merged across experimental days ("merged subject data") to facilitate comparison with other studies (Figure 4.7). These results were used to test our assumption regarding the correlation between the number of subjects in a database and the number of significant comparisons (Table 4.5). Although a strong correlation was observed between the number of subjects and our significance metric, it was not statistically significant. Nonetheless, Table 4.5 indicates that a database with only nine subjects is insufficient for significance testing. We therefore recommend using databases with large numbers of subjects, such as Physionet or Giga, for comparing BCI systems. Further investigation of our assumption will require additional open-access MI EEG databases.

We also wish to emphasize that our experiments used artifact-filtered EEG data, in contrast to previous studies on the investigated neural networks [31], [40], [42], [75], which included only bandpass filtering and standardization prior to classification. In our signal processing step, we applied a fifth-order bandpass Butterworth filter with a range of 1 to 45 Hz, and utilized the FASTER algorithm [59] to detect and remove artifacts associated with eye movements and muscle activity. This is crucial to ensure that classification is performed on pure EEG signals rather than artifacts, because it has been demonstrated in [99] that electromyography can be successfully used for BCI purposes.

Many studies investigating the effects of transfer learning have utilized datasets without artifact filtering [94], [96]–[98], [104]. Our findings demonstrate that, even after artifact filtering, the implementation of transfer learning on databases with large numbers of subjects, such as Physionet and Giga, significantly enhances the accuracy of neural network classifications relative to within-subject classifications (Figure 4.6A,B). We also showed that Deep ConvNet exhibited the greatest improvement from transfer learning across all databases (Table 4.4). In contrast, Shallow ConvNet achieved the highest performance according to our "improvement from chance level" metric for all transfer-learning-trained neural networks (Table 4.3). Nevertheless, the differences between the ConvNets were insignificant concerning the Physionet and Giga databases (Figure 4.6A,B). In within-subject training mode, Deep ConvNet exhibited suboptimal performance, which may be attributed to an insufficient quantity of training data, a crucial factor for effective training of deep neural networks.

Our results highlight the importance of considering multiple factors when ranking the performance of neural networks. Relying solely on accuracy differences between networks and using unfiltered datasets with small numbers of subjects may lead to inconclusive results.

In addition to our findings, it is important to acknowledge the limitations of our research. Only a few neural networks were selected from the EEGNet family (Table 4.1) to shrink down the computational time. While it would be valuable to expand this comparison in future studies, the inclusion of additional networks may result in less significant findings due to the Bonferroni correction. Furthermore, several limitations were identified within the databases used. Only two databases, Physionet and Giga, were found to have more than 20 subjects. The TTK and BCI Competition IV 2a datasets were extended using our independent days configuration. The databases were recorded using different paradigms and contain varying amounts and types of motor imagery tasks. Additionally, they were recorded using different EEG amplifier systems with varying numbers of electrodes. As such, the consistency of the databases cannot be guaranteed. The aforementioned limitations may also have contributed to the observed variability in the classification results of the neural networks.

In future research, it would be worthwhile to explore the potential of transfer learning using data from multiple databases. However, this approach presents challenges due to variations in recording equipment and methodology across datasets, including differences

in the position and number of electrodes, as well as sampling frequency. These issues must be addressed to facilitate effective transfer learning using data from multiple sources.

4.5. Conclusions

In this study, we conducted a critical comparison of neural networks from the EEGNet family, including Shallow ConvNet, Deep ConvNet, EEGNet, EEGNet Fusion, and MI-EEGNet, for the classification of MI EEG signals. Comparisons were performed using the BCI Competition IV 2a database as well as the Giga and Physionet databases, which comprise data from large numbers of subjects. Our TTK dataset was also utilized. Within-subject and transfer learning classifications were performed for each combination of database configuration and neural network, with all results subjected to five-fold cross-validation. Classification was performed on signals that had been cleaned of artifacts using the FASTER algorithm.

To our knowledge, this is the first study to compare neural networks from the EEGNet family on artifact-filtered databases comprising large numbers of subjects ($>$20) using cross-validated results. We demonstrated that transfer learning can improve classification performance even on artifact-filtered MI EEG data. To rank the performance of the neural networks, we introduced two metrics: one measuring improvement in accuracy relative to chance level and the other assessing improvement in classification performance achieved through transfer learning. These metrics indicated that Shallow ConvNet (0.2721, 0.0519) and Deep ConvNet (0.2598, 0.1075) outperformed more recently published networks from the EEGNet family. Finally, we showed that databases with small numbers of subjects ($\leq$10) are insufficient for statistically significant comparison of BCI systems.

10.15774/PPKE.ITK.2024.001

Chapter 5

Summary

This chapter presents a summary of the novel scientific findings in the form of thesis statements, articulated in both English and Hungarian.

5.1. New Scientific Results

Thesis group I – Development and Testing of a Real-Time Working BCI System
Corresponding publication: [J1]

Thesis I: *I developed a novel feature extraction and classification pipeline, utilizing Fast Fourier Transformation and Support Vector Machine algorithms for real-time processing and classification of motor imagery EEG signals for Brain-Computer Interface purposes.*

Thesis Ia: *I compared my implemented range40 feature extraction method, combined with my Voting SVM classifier, to the state-of-the-art EEGNet using the Physionet dataset and found that it significantly outperformed it according to the Wilcoxon statistical test.*

The range40 feature extraction method calculates the absolute of the Fast Fourier Transformation from a given EEG window and averages the values in 2 Hz wide frequency ranges (2-4 Hz, 4-6 Hz, ..., 38-40 Hz) for each EEG channel. The 19 $\times$ *channel number* generated features are used to train 19 RBF kernelled SVMs. Each SVM learned distinct characteristics of brain signals concerning the 2 Hz wide frequency ranges. Each SVM made its own decision, and the final decision was generated as the max vote of the SVM units. This ensemble SVM classifier is called as Voting SVM.

Thesis Ib: *I developed a unique control protocol, called the Toggle Switch, to extend the 2-class output of my BCI System to control a video game requiring 4 commands. My method circulates active control commands one after the other during active motor imagery till the subject selects the required command by initiating the calm mental state. This approach can easily be extended to have more than four control commands.*

Thesis Ic: *With the aid of my complete BCI System, I successfully conducted a total of 59 video game control experiments, involving two pilots diagnosed with C5 or higher spinal cord lesions. The results, in terms of online gameplay, were comparable to those of other teams participating in Cybathlon 2020.*

Thesis group II – Deep Comparisons of Neural Networks from the EEGNet Family
Corresponding publication: [J2]

Thesis II: *I selected and compared the classification and transfer learning capabilities of Shallow ConvNet, Deep ConvNet, EEGNet, EEGNet Fusion, and MI-EEGNet on artifact-rejected EEG data from four databases with varying numbers of subjects.*

Thesis IIa: *I showed that transfer learning on the selected neural networks can significantly improve classification accuracy, even after artifact rejection, compared to within-subject classification.*

Thesis IIb: *I also demonstrated that significant comparison cannot be evaluated on databases with less than or equal to 10 subjects.*

Thesis IIc: *In order to compare the neural networks, I used two metrics, "Improvement from chance level" and "Improvement by transfer learning". These metrics indicated that Shallow ConvNet and Deep ConvNet outperformed more recently published networks from the EEGNet family and highlighted the importance of considering multiple factors when ranking the performance of neural networks beyond generally used accuracy differences between networks.*

5.2. Új Tudományos Eredmények

I. Tézis csoport – Valós időben működő Agy-Számítógép Kapcsolat rendszer fejlesztése és tesztelése

Kapcsolódó publikáció: [J1]

I. Tézis *Kifejlesztettem egy új jellemzőkinyerési és osztályozási folyamatrendszert, mely gyors Fourier-transzformáció és Support Vector Machine algoritmusok felhasználásával valós időben feldolgozza és osztályozza az elképzelt motoros mozgásokhoz tartozó Elektroencefalogramokat Agy-Számítógép Kapcsolat vezérlésének céljából.*

Ia. Tézis *Összehasonlítottam az általam fejlesztett range40 jellemző kinyerési metódussal kombinált Voting SVM osztályozó rendszert a korszerű EEGNet algoritmussal a Physionet-es adatbázis felhasználásával, melynek során a Wilcoxon statisztikai teszt alkalmazásával a saját rendszerem szignifikánsan jobb eredményt mutatott.*

Ib. Tézis *Kifejlesztettem egy egyedi vezérlési protokollt, amely az Agy-Számítógép Kapcsolati rendszer 2 osztályú kimenetét 4 osztállyá alakítja, hogy irányítani lehessen egy 4 bementet váró számítógépes játékot. A rendszer aktív elképzelt mozgás esetén a vezérlő parancsokat egymás után cirkuláltatja mindaddig, amíg a felhasználó a nyugalmi állapot aktivizálásával ki nem választ egyet. Ez a módszer könnyen kiterjeszthető négynél több vezérlési parancs kiadására is.*

Ic. Tézis *Az elkészült Agy-Számítógép kapcsolati rendszer felhasználásával 59 videójáték vezérlési kísérletet végeztem két C5 vagy magasabb nyaki csigolya sérüléssel diagnosztizált kísérleti alany bevonásával. A játék irányítási eredményei összehasonlíthatóak a 2020-ban megrendezett Cybathlon versenyen résztvevő csapatok publikált eredményeivel.*

II. Tézis csoport – Az EEGNet család neurális hálózatainak kritikai összehasonlítása
Kapcsolódó publikáció: [J2]

II. Tézis *Kiválasztottam a Shallow ConvNet, Deep ConvNet, EEGNet, EEGNet Fusion és MI-EEGNet neurális hálózatokat és összehasonlítottam az osztályozó és transzfer tanulás képességeiket artefakt-szűrt EEG adatokon, melyek 4 különböző alanyszámú adatbázisokból származnak.*

IIa. Tézis *Megmutattam, hogy artefakt eltávolítást követve a transzfer tanulás alkalmazásával a kiválasztott neurális hálózatokon szignifikánsan jobb osztályozási eredmény érhető el, mintha csak alanyonkénti osztályozást végeznénk.*

IIb. Tézis *Az összehasonlítás során szintén demonstráltam, hogy 10-nél kevesebb alanyt tartalmazó adatbázison nem lehet szignifikáns összehasonlítást végezni.*

IIc. Tézis *A neurális hálózatok összehasonlításához két metrikát használtam, a „Véletlen szinttől történő javulás" és a „Transzfer tanulás általi javulás". Ezek a metrikák azt mutatták, hogy a Shallow ConvNet és a Deep ConvNet hálózatok jobban teljesítettek, mint az EEGNet család újabban publikált tagjai. Az eredmények rámutatnak arra, hogy a neurális hálózatok teljesítményének rangsorolásakor több tényezőt is figyelembe kell venni az általánosan használt osztályozási pontosság összehasonlításán kívül.*

5.3. Potential Applications and Benefits

The BCI System was designed for a concrete application called the BCI discipline in the Cybathlon 2020 competition, where pilots with quadriplegia compete in a car-racing-like computer game by controlling their avatar using well-timed imagined mental commands recorded by EEG.

In addition, this work was prepared with the professional support of the Doctoral Student Scholarship Program of the Co-operative Doctoral Program (hungarian abbreviation: KDP) of the Ministry of Innovation and Technology financed from the National Research, Development and Innovation Fund. The so-called KDP grant aims to implement scientific research to industrial purposes. Therefore the gained knowledge was transferred to the domain of electromyographycal signal processing domain, where small, portable, affordable EMG armband was used. The complete study is presented in [Au4] and [Au5].

10.15774/PPKE.ITK.2024.001

I highlighted by the comparison of members of the EEGNet family, that it is vital for presenting new classification methods for EEG signal processing to use databases with large numbers of subjects, such as Physionet or Giga. I also highlighted the importance of considering multiple factors when ranking the performance of neural networks. Relying solely on accuracy differences between networks and using unfiltered datasets with small numbers of subjects may lead to inconclusive results. Ideally these findings could lead to a new comparison procedure when a new neural network is presented for EEG signal classification.

Journal publications of the thesis

[J1] **Cs. Köllőd**, A. Adolf, G. Márton, M. Wahdow, W. Fadel, and I. Ulbert, "Closed loop BCI system for Cybathlon 2020", *Brain-Computer Interfaces*, 10th vol., 2nd no., pp. 114–128, 2023. DOI: 10.1080/2326263X.2023.2254463.

[J2] **Cs. Köllőd**, A. Adolf, K. Iván, G. Márton, and I. Ulbert, "Deep Comparisons of Neural Networks from the EEGNet Family", *Electronics*, 12th vol., 12th no., p. 2743, 2023. DOI: 10.3390/electronics12122743.

Other publications of the author

[Au1] M. Wahdow, M. Alnaanah, W. Fadel, A. Adolf, **Cs. Kollod**, and I. Ulbert, "Multi frequency band fusion method for EEG signal classification", *Signal, Image and Video Processing*, 2022. DOI: 10.1007/s11760-022-02399-6.

[Au2] W. Fadel, **Cs. Kollod**, M. Wahdow, Y. Ibrahim, and I. Ulbert, "Multi-Class Classification of Motor Imagery EEG Signals Using Image-Based Deep Recurrent Convolutional Neural Network", in *2020 8th International Winter Conference on Brain-Computer Interface (BCI)*, 2020, pp. 1–4. DOI: 10.1109/BCI48061.2020.9061622.

[Au3] W. Fadel, M. Wahdow, **Cs. Kollod**, G. Marton, and I. Ulbert, "Chessboard EEG Images Classification for BCI Systems Using Deep Neural Network", in *Bio-inspired Information and Communication Technologies*, Y. Chen, T. Nakano, L. Lin, M. U. Mahfuz, and W. Guo, Eds., Lecture Notes of the Institute for Computer Sciences, Social Informatics and Telecommunications Engineering ser., vol. 329,

Cham: Springer International Publishing, 2020, pp. 97–104. DOI: 10.1007/978-3-030-57115-3_8.

[Au4] N. J. Eftimiu, **Cs. Köllőd**, I. Ulbert, and G. Márton, "A Surface Electromyography Dataset for Hand Gesture Recognition", in *2022 IEEE 20th Jubilee International Symposium on Intelligent Systems and Informatics (SISY)*, 2022, pp. 115–120. DOI: 10.1109/SISY56759.2022.10036305.

[Au5] **Cs. Köllőd**, N. J. Eftimiu, G. Márton, and I. Ulbert, "Classification of Semi-Automated Labeled MindRove Armband Recorded EMG Data", in *2022 IEEE 22nd International Symposium on Computational Intelligence and Informatics and 8th IEEE International Conference on Recent Achievements in Mechatronics, Automation, Computer Science and Robotics (CINTI-MACRo)*, 2022, pp. 381–386. DOI: 10.1109/CINTI-MACRo57952.2022.10029540.

[Au6] **Cs. Köllőd**, A. Adolf, G. Márton, M. Wahdow, W. Fadel, and I. Ulbert, *TTK dataset - 4 class Motor-Imagery EEG*, 2022, https://hdl.handle.net/21.15109/CONCORDA/UOQQVK.

Bibliography

[1] J. R. Wolpaw, N. Birbaumer, D. J. McFarland, G. Pfurtscheller, and T. M. Vaughan, "Brain–computer interfaces for communication and control", *Clinical Neurophysiology*, 113th vol., 6th no., pp. 767–791, 2002. DOI: 10.1016/S1388-2457(02)00057-3.

[2] G. Karmos, B. Dombovári, I. Ulbert, R. Csercsa, R. Fiáth, and D. Horváth, *Electrophysiological Methods for the Study of the Nervous- and Muscular-Systems*, eng. Budapest, Hungary: Semmelweis Egyetem, Dialóg Campus Kiadó, Pázmány Péter Katolikus Egyetem, 2011.

[3] C. Klaes, "Chapter 28 - Invasive Brain-Computer Interfaces and Neural Recordings From Humans", in *Handbook of Behavioral Neuroscience*, Handbook of Neural Plasticity Techniques ser., D. Manahan-Vaughan, Ed., vol. 28, Elsevier, 2018, pp. 527–539. DOI: 10.1016/B978-0-12-812028-6.00028-8.

[4] A. K. Engel, C. K. E. Moll, I. Fried, and G. A. Ojemann, "Invasive recordings from the human brain: Clinical insights and beyond", *Nature Reviews Neuroscience*, 6th vol., 1st no., pp. 35–47, 2005. DOI: 10.1038/nrn1585.

[5] S. Waldert, T. Pistohl, C. Braun, T. Ball, A. Aertsen, and C. Mehring, "A review on directional information in neural signals for brain-machine interfaces", *Journal of Physiology-Paris*, Neurorobotics, 103rd vol., 3rd no., pp. 244–254, 2009. DOI: 10.1016/j.jphysparis.2009.08.007.

[6] L. F. Nicolas-Alonso and J. Gomez-Gil, "Brain Computer Interfaces, a Review", *Sensors*, 12th vol., 2nd no., pp. 1211–1279, 2012. DOI: 10.3390/s120201211.

[7] G. Karmos, B. Dombovári, I. Ulbert, *et al.*, *Neural Interfaces and Prostheses*, eng. Budapest, Hungary: Semmelweis Egyetem, Dialóg Campus Kiadó, Pázmány Péter Katolikus Egyetem, 2011.

[8] M. Ahn, H. Cho, S. Ahn, and S. C. Jun, "High Theta and Low Alpha Powers May Be Indicative of BCI-Illiteracy in Motor Imagery", *PLOS ONE*, 8th vol., 11th no., e80886, 2013. DOI: 10.1371/journal.pone.0080886.

[9] N. Rustamov, J. Humphries, A. Carter, and E. C. Leuthardt, "Theta–gamma coupling as a cortical biomarker of brain–computer interface-mediated motor recovery in chronic stroke", *Brain Communications*, 4th vol., 3rd no., fcac136, 2022. DOI: 10.1093/braincomms/fcac136.

[10] G. Pfurtscheller and R. Cooper, "Frequency dependence of the transmission of the EEG from cortex to scalp", *Electroencephalography and Clinical Neurophysiology*, 38th vol., 1st no., pp. 93–96, 1975. DOI: 10.1016/0013-4694(75)90215-1.

[11] J. G. Stinstra and M. J. Peters, "The volume conductor may act as a temporal filter on the ECG and EEG", en, *Medical and Biological Engineering and Computing*, 36th vol., 6th no., pp. 711–716, 1998. DOI: 10.1007/BF02518873.

[12] G. Bin, X. Gao, Y. Wang, B. Hong, and S. Gao, "VEP-based brain-computer interfaces: Time, frequency, and code modulations [Research Frontier]", *IEEE Computational Intelligence Magazine*, 4th vol., 4th no., pp. 22–26, 2009. DOI: 10.1109/MCI.2009.934562.

[13] C. Guger, S. Daban, E. Sellers, *et al.*, "How many people are able to control a P300-based brain–computer interface (BCI)?", *Neuroscience Letters*, 462nd vol., 1st no., pp. 94–98, 2009. DOI: 10.1016/j.neulet.2009.06.045.

[14] E. Sellers, A. Kubler, and E. Donchin, "Brain-computer interface research at the university of south Florida cognitive psychophysiology laboratory: The P300 speller", *IEEE Transactions on Neural Systems and Rehabilitation Engineering*, 14th vol., 2nd no., pp. 221–224, 2006. DOI: 10.1109/TNSRE.2006.875580.

[15] B. Hudgins, P. Parker, and R. Scott, "A new strategy for multifunction myoelectric control", *IEEE Transactions on Biomedical Engineering*, 40th vol., 1st no., pp. 82–94, 1993. DOI: 10.1109/10.204774.

[16] P. Geethanjali, Y. K. Mohan, and J. Sen, "Time domain Feature extraction and classification of EEG data for Brain Computer Interface", in *2012 9th International Conference on Fuzzy Systems and Knowledge Discovery*, 2012, pp. 1136–1139. DOI: 10.1109/FSKD.2012.6234336.

[17] J. Abougharbia, O. Attallah, M. Tamazin, and A. Nasser, "A Novel BCI System Based on Hybrid Features for Classifying Motor Imagery Tasks", in *2019 Ninth International Conference on Image Processing Theory, Tools and Applications (IPTA)*, 2019, pp. 1–6. DOI: 10.1109/IPTA.2019.8936119.

[18] M. Tavakolan, Z. Frehlick, X. Yong, and C. Menon, "Classifying three imaginary states of the same upper extremity using time-domain features", *PLOS ONE*, 12th vol., 3rd no., e0174161, 2017. DOI: 10.1371/journal.pone.0174161.

[19] C. W. Anderson and Z. Sijercic, "Classification of EEG signals from four subjects during five mental tasks", in *Solving engineering problems with neural networks: proceedings of the conference on engineering applications in neural networks*, Turkey, 1996, pp. 407–414.

[20] H. Ramoser, J. Muller-Gerking, and G. Pfurtscheller, "Optimal spatial filtering of single trial EEG during imagined hand movement", *IEEE Transactions on Rehabilitation Engineering*, 8th vol., 4th no., pp. 441–446, 2000. DOI: 10.1109/86.895946.

[21] F. Lotte and C. Guan, "Regularizing Common Spatial Patterns to Improve BCI Designs: Unified Theory and New Algorithms", *IEEE Transactions on Biomedical Engineering*, 58th vol., 2nd no., pp. 355–362, 2011. DOI: 10.1109/TBME.2010.2082539.

[22] K. K. Ang, Z. Y. Chin, C. Wang, C. Guan, and H. Zhang, "Filter Bank Common Spatial Pattern Algorithm on BCI Competition IV Datasets 2a and 2b", English, *Frontiers in Neuroscience*, 6th vol., 39th no., 2012. DOI: 10.3389/fnins.2012.00039.

[23] P. Welch, "The use of fast Fourier transform for the estimation of power spectra: A method based on time averaging over short, modified periodograms", *IEEE Transactions on Audio and Electroacoustics*, 15th vol., 2nd no., pp. 70–73, 1967. DOI: 10.1109/tau.1967.1161901.

[24] A. S. Al-Fahoum and A. A. Al-Fraihat, "Methods of EEG Signal Features Extraction Using Linear Analysis in Frequency and Time-Frequency Domains", *International Scholarly Research Notices*, 2014th vol., e730218, 2014. DOI: 10.1155/2014/730218.

[25] G. Xu, X. Shen, S. Chen, *et al.*, "A Deep Transfer Convolutional Neural Network Framework for EEG Signal Classification", *IEEE Access*, 7th vol., pp. 112 767–112 776, 2019. DOI: 10.1109/access.2019.2930958.

[26] Y. R. Tabar and U. Halici, "A novel deep learning approach for classification of EEG motor imagery signals", *Journal of Neural Engineering*, 14th vol., 16003rd no., 2017. DOI: 10.1088/1741-2560/14/1/016003.

[27] Y. Han, B. Wang, J. Luo, L. Li, and X. Li, "A classification method for EEG motor imagery signals based on parallel convolutional neural network", *Biomedical Signal Processing and Control*, 71st vol., 103190th no., 2022. DOI: 10.1016/j.bspc.2021.103190.

[28] B. E. Boser, I. M. Guyon, and V. N. Vapnik, "A training algorithm for optimal margin classifiers", in *Proceedings of the fifth annual workshop on Computational learning theory*, COLT '92 ser., New York, NY, USA: Association for Computing Machinery, 1992, pp. 144–152. DOI: 10.1145/130385.130401.

[29] I. Goodfellow, Y. Bengio, and A. Courville, *Deep Learning*. MIT Press, 2006.

[30] S. Haykin, *Neural Networks and Learning Machines*, 3rd ed. New Jersey: Pearson Education, Inc., 2009.

[31] V. J. Lawhern, A. J. Solon, N. R. Waytowich, S. M. Gordon, C. P. Hung, and B. J. Lance, "EEGNet: A compact convolutional neural network for EEG-based brain–computer interfaces", *Journal of Neural Engineering*, 15th vol., 5th no., p. 17, 2018. DOI: 10.1088/1741-2552/aace8c.

[32] L. A. Farwell and E. Donchin, "Talking off the top of your head: Toward a mental prosthesis utilizing event-related brain potentials", *Electroencephalography and Clinical Neurophysiology*, 70th vol., 6th no., pp. 510–523, 1988. DOI: 10.1016/0013-4694(88)90149-6.

[33] J. R. Wolpaw, D. J. McFarland, G. W. Neat, and C. A. Forneris, "An EEG-based brain-computer interface for cursor control", *Electroencephalography and Clinical Neurophysiology*, 78th vol., 3rd no., pp. 252–259, 1991. DOI: 10.1016/0013-4694(91)90040-B.

[34] R. Leeb, S. Perdikis, L. Tonin, *et al.*, "Transferring brain–computer interfaces beyond the laboratory: Successful application control for motor-disabled users", *Artificial Intelligence in Medicine*, Special Issue: Brain-computer interfacing, 59th vol., 2nd no., pp. 121–132, 2013. DOI: 10.1016/j.artmed.2013.08.004.

[35] R. Riener and L. J. Seward, "Cybathlon 2016", in *2014 IEEE International Conference on Systems, Man, and Cybernetics (SMC)*, 2014, pp. 2792–2794. DOI: 10.1109/SMC.2014.6974351.

[36] S. Perdikis, L. Tonin, S. Saeedi, C. Schneider, and J. d. R. Millán, "The Cybathlon BCI race: Successful longitudinal mutual learning with two tetraplegic users", *PLOS Biology*, 16th vol., 5th no., p. 28, 2018. DOI: 10.1371/journal.pbio.2003787.

[37] S. Tortora, G. Beraldo, F. Bettella, *et al.*, "Neural correlates of user learning during long-term BCI training for the Cybathlon competition", *Journal of NeuroEngineering and Rehabilitation*, 19th vol., 69th no., 2022. DOI: 10.1186/s12984-022-01047-x.

[38] K. Statthaler, A. Schwarz, D. Steyrl, *et al.*, "Cybathlon experiences of the Graz BCI racing team Mirage91 in the brain-computer interface discipline", *Journal of NeuroEngineering and Rehabilitation*, 14th vol., 129th no., p. 16, 2017. DOI: 10.1186/s12984-017-0344-9.

[39] L. Hehenberger, R. J. Kobler, C. Lopes-Dias, *et al.*, "Long-Term Mutual Training for the CYBATHLON BCI Race With a Tetraplegic Pilot: A Case Study on Inter-Session Transfer and Intra-Session Adaptation", *Frontiers in Human Neuroscience*, 15th vol., 635777th no., p. 15, 2021. DOI: 10.3389/fnhum.2021.635777.

[40] M. Riyad, M. Khalil, and A. Adib, "MI-EEGNET: A novel convolutional neural network for motor imagery classification", *Journal of Neuroscience Methods*, 353rd vol., 109037th no., 2021. DOI: 10.1016/j.jneumeth.2020.109037.

[41] D. Zhang, L. Yao, X. Zhang, S. Wang, W. Chen, and R. Boots, "EEG-based Intention Recognition from Spatio-Temporal Representations via Cascade and Parallel Convolutional Recurrent Neural Networks", *arXiv:1708.06578 [cs, q-bio]*, 2017.

[42] K. Roots, Y. Muhammad, and N. Muhammad, "Fusion Convolutional Neural Network for Cross-Subject EEG Motor Imagery Classification", *Computers*, 9th vol., 72nd no., 2020. DOI: 10.3390/computers9030072.

[43] N. Gedik, "Classification of Right and Left-Hand Movement Using Multi-Resolution Analysis Method", *International Journal of Biomedical and Biological Engineering*, 15th vol., 1st no., pp. 6–9, 2021.

[44] H. Varsehi and S. M. P. Firoozabadi, "An EEG channel selection method for motor imagery based brain–computer interface and neurofeedback using Granger causality", *Neural Networks*, 133rd vol., pp. 193–206, 2021. DOI: 10.1016/j.neunet.2020.11.002.

[45] D. Gwon and M. Ahn, "Alpha and High gamma phase amplitude coupling during motor imagery and Weighted Cross-Frequency Coupling to extract discriminative cross-frequency patterns", *NeuroImage*, p. 118 403, 2021. DOI: 10.1016/j.neuroimage.2021.118403.

[46] Y. Huang, J. Jin, R. Xu, Y. Miao, C. Liu, and A. Cichocki, "Multi-view optimization of time-frequency common spatial patterns for brain-computer interfaces", *Journal of Neuroscience Methods*, 365th vol., p. 109 378, 2022. DOI: 10.1016/j.jneumeth.2021.109378.

[47] J. Jin, Y. Miao, I. Daly, C. Zuo, D. Hu, and A. Cichocki, "Correlation-based channel selection and regularized feature optimization for MI-based BCI", *Neural Networks*, 118th vol., pp. 262–270, 2019. DOI: 10.1016/j.neunet.2019.07.008.

[48] D. Li, J. Xu, J. Wang, X. Fang, and J. Ying, "A Multi-Scale Fusion Convolutional Neural Network based on Attention Mechanism for the Visualization Analysis of EEG Signals Decoding", *IEEE Transactions on Neural Systems and Rehabilitation Engineering*, pp. 1–1, 2020. DOI: 10.1109/tnsre.2020.3037326.

[49] B. Blankertz, K.-R. Muller, G. Curio, *et al.*, "The BCI competition 2003: Progress and perspectives in detection and discrimination of EEG single trials", *IEEE Transactions on Biomedical Engineering*, 51st vol., 6th no., pp. 1044–1051, 2004. DOI: 10.1109/TBME.2004.826692.

[50] B. Blankertz, K.-R. Muller, D. Krusienski, *et al.*, "The BCI competition III: Validating alternative approaches to actual BCI problems", *IEEE Transactions on Neural Systems and Rehabilitation Engineering*, 14th vol., 2nd no., pp. 153–159, 2006. DOI: 10.1109/TBME.2004.826692.

[51] P. Sajda, A. Gerson, K.-R. Muller, B. Blankertz, and L. Parra, "A data analysis competition to evaluate machine learning algorithms for use in brain-computer interfaces", *IEEE Transactions on Neural Systems and Rehabilitation Engineering*, 11th vol., 2nd no., pp. 184–185, 2003. DOI: 10.1109/TNSRE.2003.814453.

[52] M. Tangermann, K.-R. Müller, A. Aertsen, *et al.*, "Review of the BCI Competition IV", *Frontiers in Neuroscience*, 6th vol., 55th no., p. 31, 2012. DOI: 10.3389/fnins.2012.00055.

[53] C.-C. Fan, H. Yang, Z.-G. Hou, Z.-L. Ni, S. Chen, and Z. Fang, "Bilinear neural network with 3-D attention for brain decoding of motor imagery movements from the human EEG", *Cognitive Neurodynamics*, 15th vol., pp. 181–189, 2020. DOI: 10.1007/s11571-020-09649-8.

[54] Goldberger Ary L., Amaral Luis A. N., Glass Leon, *et al.*, "PhysioBank, PhysioToolkit, and PhysioNet", *Circulation*, 101st vol., 23rd no., pp. 215–220, 2000. DOI: 10.1161/01.CIR.101.23.e215.

[55] A. Bria, C. Marrocco, and F. Tortorella, "Sinc-based convolutional neural networks for EEG-BCI-based motor imagery classification", *arXiv:2101.10846 [eess]*, 2021.

[56] G. Schalk, D. J. McFarland, T. Hinterberger, N. Birbaumer, and J. R. Wolpaw, "BCI2000: A general-purpose brain-computer interface (BCI) system", eng, *IEEE transactions on bio-medical engineering*, 51st vol., 6th no., pp. 1034–1043, 2004. DOI: 10.1109/TBME.2004.827072.

[57] A. Gramfort, M. Luessi, E. Larson, *et al.*, "MEG and EEG data analysis with MNE-Python", English, *Frontiers in Neuroscience*, 7th vol., 2013. DOI: 10.3389/fnins.2013.00267.

[58] M. Abadi, A. Agarwal, P. Barham, *et al.*, "TensorFlow: Large-Scale Machine Learning on Heterogeneous Distributed Systems", *arXiv:1603.04467 [cs]*, 2016.

[59] H. Nolan, R. Whelan, and R. B. Reilly, "FASTER: Fully Automated Statistical Thresholding for EEG artifact Rejection", *Journal of Neuroscience Methods*, 192nd vol., 1st no., pp. 152–162, 2010. DOI: 10.1016/j.jneumeth.2010.07.015.

[60] M. v. Vliet, *Wmvanvliet/mne-faster: First official release*, 2021. DOI: 10.5281/zenodo.5112399.

[61] F. Pedregosa, G. Varoquaux, A. Gramfort, *et al.*, "Scikit-learn: Machine Learning in Python", *Journal of Machine Learning Research*, 12th vol., 85th no., pp. 2825–2830, 2011.

[62] K. P. Thomas, C. Guan, C. T. Lau, A. P. Vinod, and K. K. Ang, "A New Discriminative Common Spatial Pattern Method for Motor Imagery Brain–Computer Interfaces", *IEEE Transactions on Biomedical Engineering*, 56th vol., 11th no., pp. 2730–2733, 2009. DOI: 10.1109/tbme.2009.2026181.

[63] M. Riyad, M. Khalil, and A. Adib, "A novel multi-scale convolutional neural network for motor imagery classification", *Biomedical Signal Processing and Control*, 68th vol., 102747th no., 2021. DOI: 10.1016/j.bspc.2021.102747.

[64] C. Benaroch, K. Sadatnejad, A. Roc, *et al.*, "Long-Term BCI Training of a Tetraplegic User: Adaptive Riemannian Classifiers and User Training", *Frontiers in Human Neuroscience*, 15th vol., 635653rd no., p. 22, 2021. DOI: 10.3389/fnhum.2021.635653.

[65] N. Robinson, T. Chouhan, E. Mihelj, *et al.*, "Design Considerations for Long Term Non-invasive Brain Computer Interface Training With Tetraplegic CYBATHLON Pilot", *Frontiers in Human Neuroscience*, 15th vol., 648275th no., p. 16, 2021. DOI: 10.3389/fnhum.2021.648275.

[66] A. Korik, K. McCreadie, N. McShane, *et al.*, "Competing at the Cybathlon championship for people with disabilities: Long-term motor imagery brain–computer interface training of a cybathlete who has tetraplegia", *Journal of NeuroEngineering and Rehabilitation*, 19th vol., 95th no., p. 22, 2022. DOI: 10.1186/s12984-022-01073-9.

[67] D. A. Blanco-Mora, A. Aldridge, C. Jorge, A. Vourvopoulos, P. Figueiredo, and S. Bermúdez i Badia, "Finding the optimal time window for increased classification accuracy during motor imagery", eng, *Proceedings of the 14th International Joint Conference on Biomedical Engineering Systems and Technologies*, pp. 144–151, 2021. DOI: 10.5220/0010316101440151.

[68] J. W. Cooley and J. W. Tukey, "An Algorithm for the Machine Calculation of Complex Fourier Series", *Mathematics of Computation*, 19th vol., 90th no., pp. 297–301, 1965. DOI: 10.2307/2003354.

[69] V. N. G. Raju, K. P. Lakshmi, V. M. Jain, A. Kalidindi, and V. Padma, "Study the Influence of Normalization/Transformation process on the Accuracy of Supervised Classification", in *2020 Third International Conference on Smart Systems and Inventive Technology (ICSSIT)*, 2020, pp. 729–735. DOI: 10.1109/icssit48917.2020.9214160.

[70] Y. Zhang, J. Liu, J. Liu, J. Sheng, and J. Lv, "EEG Recognition of Motor Imagery Based on SVM Ensemble", in *2018 5th International Conference on Systems and Informatics (ICSAI)*, 2018, pp. 866–870. DOI: 10.1109/ICSAI.2018.8599464.

[71] T. Stenner, C. Boulay, M. Grivich, *et al.*, *Sccn/liblsl: V1.15.1 - ASIO updated*, 2021. DOI: 10.5281/zenodo.5415959.

[72] G. R. Müller-Putz, D. Coyle, F. Lotte, J. Jin, and D. Steyrl, "Editorial: Long Term User Training and Preparation to Succeed in a Closed-Loop BCI Competition", *Frontiers in Human Neuroscience*, 16th vol., 2022. DOI: 10.3389/fnhum.2022.869700.

[73] D. Novak, R. Sigrist, N. J. Gerig, *et al.*, "Benchmarking Brain-Computer Interfaces Outside the Laboratory: The Cybathlon 2016", *Frontiers in Neuroscience*, 11th vol., 756th no., p. 14, 2018. DOI: 10.3389/fnins.2017.00756.

[74] F. Turi, M. Clerc, and T. Papadopoulo, "Long Multi-Stage Training for a Motor-Impaired User in a BCI Competition", *Frontiers in Human Neuroscience*, 15th vol., 647908th no., 2021. DOI: 10.3389/fnhum.2021.647908.

[75] R. T. Schirrmeister, J. T. Springenberg, L. D. J. Fiederer, *et al.*, "Deep learning with convolutional neural networks for EEG decoding and visualization", *Human Brain Mapping*, 38th vol., 11th no., pp. 5391–5420, 2017. DOI: 10.1002/hbm.23730.

[76] M.-H. Lee, O.-Y. Kwon, Y.-J. Kim, *et al.*, "EEG dataset and OpenBMI toolbox for three BCI paradigms: An investigation into BCI illiteracy", *GigaScience*, 8th vol., 5th no., p. 16, 2019. DOI: 10.1093/gigascience/giz002.

[77] B. Blankertz, G. Dornhege, M. Krauledat, K.-R. Müller, and G. Curio, "The non-invasive Berlin Brain–Computer Interface: Fast acquisition of effective performance in untrained subjects", *NeuroImage*, 37th vol., 2nd no., pp. 539–550, 2007. DOI: 10.1016/j.neuroimage.2007.01.051.

[78] A. Barachant, S. Bonnet, M. Congedo, and C. Jutten, "Riemannian Geometry Applied to BCI Classification", in *Latent Variable Analysis and Signal Separation*, V. Vigneron, V. Zarzoso, E. Moreau, R. Gribonval, and E. Vincent, Eds., Lecture Notes in Computer Science ser., Berlin, Heidelberg: Springer, 2010, pp. 629–636. DOI: 10.1007/978-3-642-15995-4_78.

[79] S. Sakhavi, C. Guan, and S. Yan, "Parallel convolutional-linear neural network for motor imagery classification", in *2015 23rd European Signal Processing Conference (EUSIPCO)*, 2015, pp. 2736–2740. DOI: 10.1109/EUSIPCO.2015.7362882.

[80] I. Sturm, S. Lapuschkin, W. Samek, and K.-R. Müller, "Interpretable deep neural networks for single-trial EEG classification", *Journal of Neuroscience Methods*, 274th vol., pp. 141–145, 2016. DOI: 10.1016/j.jneumeth.2016.10.008.

[81] W. Huang, Y. Xue, L. Hu, and H. Liuli, "S-EEGNet: Electroencephalogram Signal Classification Based on a Separable Convolution Neural Network With Bilinear Interpolation", *IEEE Access*, 8th vol., pp. 131 636–131 646, 2020. DOI: 10.1109/ACCESS.2020.3009665.

[82] Y. K. Musallam, N. I. AlFassam, G. Muhammad, *et al.*, "Electroencephalography-based motor imagery classification using temporal convolutional network fusion", *Biomedical Signal Processing and Control*, 69th vol., 102826th no., 2021. DOI: 10.1016/j.bspc.2021.102826.

[83] X. Deng, B. Zhang, N. Yu, K. Liu, and K. Sun, "Advanced TSGL-EEGNet for Motor Imagery EEG-Based Brain-Computer Interfaces", *IEEE Access*, 9th vol., pp. 25 118–25 130, 2021. DOI: 10.1109/ACCESS.2021.3056088.

[84] W. Ma, Y. Gong, G. Zhou, Y. Liu, L. Zhang, and B. He, "A channel-mixing convolutional neural network for motor imagery EEG decoding and feature visualization", *Biomedical Signal Processing and Control*, 70th vol., 103021st no., 2021. DOI: 10.1016/j.bspc.2021.103021.

[85] H. Altaheri, G. Muhammad, and M. Alsulaiman, "Physics-inform attention temporal convolutional network for EEG-based motor imagery classification", *IEEE Transactions on Industrial Informatics*, 19th vol., 2nd no., pp. 2049–2058, 2022. DOI: 10.1109/TII.2022.3197419.

[86] H. Li, M. Ding, R. Zhang, and C. Xiu, "Motor imagery EEG classification algorithm based on CNN-LSTM feature fusion network", *Biomedical Signal Processing and Control*, 72nd vol., 103342nd no., 2022. DOI: 10.1016/j.bspc.2021.103342.

[87] H. Li, H. Chen, Z. Jia, R. Zhang, and F. Yin, "A parallel multi-scale time-frequency block convolutional neural network based on channel attention module for motor imagery classification", *Biomedical Signal Processing and Control*, 79th vol., 104066th no., 2022. DOI: 10.1016/j.bspc.2022.104066.

[88] X. Liu, R. Shi, Q. Hui, *et al.*, "TCACNet: Temporal and channel attention convolutional network for motor imagery classification of EEG-based BCI", *Information Processing & Management*, 59th vol., 103001st no., 2022. DOI: 10.1016/j.ipm.2022.103001.

[89] H. Yao, K. Liu, X. Deng, X. Tang, and H. Yu, "FB-EEGNet: A fusion neural network across multi-stimulus for SSVEP target detection", *Journal of Neuroscience Methods*, 379th vol., 109674th no., 2022. DOI: 10.1016/j.jneumeth.2022.109674.

[90] C. Gao, W. Liu, and X. Yang, "Convolutional neural network and riemannian geometry hybrid approach for motor imagery classification", *Neurocomputing*, 507th vol., pp. 180–190, 2022. DOI: 10.1016/j.neucom.2022.08.024.

[91] Z. Dokur and T. Olmez, "Classification of motor imagery electroencephalogram signals by using a divergence based convolutional neural network", *Applied Soft Computing*, 113th vol., 107881st no., 2021. DOI: 10.1016/j.asoc.2021.107881.

[92] X. Jia, Y. Song, L. Yang, and L. Xie, "Joint spatial and temporal features extraction for multi-classification of motor imagery EEG", *Biomedical Signal Processing and Control*, 71st vol., 103247th no., 2022. DOI: 10.1016/j.bspc.2021.103247.

[93] X. Jia, Y. Song, and L. Xie, "Excellent fine-tuning: From specific-subject classification to cross-task classification for motor imagery", *Biomedical Signal Processing and Control*, 79th vol., 104051st no., 2023. DOI: 10.1016/j.bspc.2022.104051.

[94] A. M. Roy, "Adaptive transfer learning-based multiscale feature fused deep convolutional neural network for EEG MI multiclassification in brain–computer interface", *Engineering Applications of Artificial Intelligence*, 116th vol., 105347th no., 2022. DOI: 10.1016/j.engappai.2022.105347.

[95] K. Weiss, T. M. Khoshgoftaar, and D. Wang, "A survey of transfer learning", *Journal of Big Data*, 3rd vol., 9th no., 2016. DOI: 10.1186/s40537-016-0043-6.

[96] Z. Khademi, F. Ebrahimi, and H. M. Kordy, "A transfer learning-based CNN and LSTM hybrid deep learning model to classify motor imagery EEG signals", *Computers in Biology and Medicine*, 143rd vol., 105288th no., 2022. DOI: 10.1016/j.compbiomed.2022.105288.

[97] F. Mattioli, C. Porcaro, and G. Baldassarre, "A 1D CNN for high accuracy classification and transfer learning in motor imagery EEG-based brain-computer interface", *Journal of Neural Engineering*, 18th vol., 66053rd no., 2022. DOI: 10.1088/1741-2552/ac4430.

[98] R. Zhang, Q. Zong, L. Dou, X. Zhao, Y. Tang, and Z. Li, "Hybrid deep neural network using transfer learning for EEG motor imagery decoding", *Biomedical Signal Processing and Control*, 63rd vol., 102144th no., 2021. DOI: 10.1016/j.bspc.2020.102144.

[99] E. Noboa, M. Rácz, L. Szűcs, P. Galambos, G. Márton, and G. Eigner, "Development of an EMG based SVM supported control solution for the PlatypOUs education mobile robot using MindRove headset", *IFAC-PapersOnLine*, 11th IFAC Symposium on Biological and Medical Systems BMS 2021, 54th vol., 15th no., pp. 304–309, 2021. DOI: 10.1016/j.ifacol.2021.10.273.

[100] E. Gibson, N. J. Lobaugh, S. Joordens, and A. R. McIntosh, "EEG variability: Task-driven or subject-driven signal of interest?", *NeuroImage*, 252nd vol., 119034th no., 2022. DOI: 10.1016/j.neuroimage.2022.119034.

[101] G. Huang, Z. Hu, W. Chen, *et al.*, "M3CV: A multi-subject, multi-session, and multi-task database for EEG-based biometrics challenge", *NeuroImage*, 264th vol., 119666th no., 2022. DOI: 10.1016/j.neuroimage.2022.119666.

[102] I. A. Castiblanco Jimenez, J. S. Gomez Acevedo, E. C. Olivetti, *et al.*, "User Engagement Comparison between Advergames and Traditional Advertising Using EEG: Does the User's Engagement Influence Purchase Intention?", *Electronics*, 12th vol., 1st no., p. 122, 2022. DOI: 10.3390/electronics12010122.

[103] L. Prechelt, "Early Stopping — But When?", in *Neural Networks: Tricks of the Trade: Second Edition*, Lecture Notes in Computer Science ser., G. Montavon, G. B. Orr, and K.-R. Müller, Eds., Berlin, Heidelberg: Springer, 2012, pp. 53–67. DOI: 10.1007/978-3-642-35289-8_5.

[104] P. Kant, S. H. Laskar, J. Hazarika, and R. Mahamune, "CWT Based Transfer Learning for Motor Imagery Classification for Brain computer Interfaces", *Journal of Neuroscience Methods*, 345th vol., 108886th no., 2020. DOI: 10.1016/j.jneumeth.2020.108886.